© 2017. Published by The Company of Biologists Ltd | Development (2017) 144, 3325-3335 doi:10.1242/dev.154864

RESEARCH ARTICLE

Pitx1 directly modulates the core limb development program to implement hindlimb identity

Stephen Nemec[1,2], Maëva Luxey[1], Deepak Jain[1,3], Aurélie Huang Sung[1], Tomi Pastinen[4] and Jacques Drouin[1,2,3,*]

ABSTRACT

Forelimbs (FLs) and hindlimbs (HLs) develop complex musculoskeletal structures that rely on the deployment of a conserved developmental program. *Pitx1*, a transcription factor gene with expression restricted to HL and absent from FL, plays an important role in generating HL features. The genomic mechanisms by which *Pitx1* effects HL identity remain poorly understood. Here, we use expression profiling and analysis of direct Pitx1 targets to characterize the HL- and FL-restricted genetic programs in mouse and situate the *Pitx1*-dependent gene network within the context of limb-specific gene regulation. We show that *Pitx1* is a crucial component of a narrow network of HL-restricted regulators, acting on a developmental program that is shared between FL and HL. Pitx1 targets sites that are in a similar chromatin state in FL and HL and controls expression of patterning genes as well as the chondrogenic program, consistent with impaired chondrogenesis in *Pitx1*$^{-/-}$ HL. These findings support a model in which multifactorial actions of a limited number of HL regulators redirect the generic limb development program in order to generate the unique structural features of the limb.

KEY WORDS: Limb specification, Regulatory network, Expression profiling, ChIPseq, Tbx5, Mouse

INTRODUCTION

In tetrapods, forelimbs (FLs) and hindlimbs (HLs) develop complex musculoskeletal structures within the framework of a common three-segment organization. Despite differences in structure and utility, the FLs and HLs of mice and humans both contain a proximal one-bone stylopod, an intermediate zeugopod segment with two bones, and a distal autopod with five digits. The arrangement of cartilage, bone, muscle and tendon within this framework, however, depends on the reproducible implementation of an underlying developmental program, and the differences in pattern between limbs arise from limb-specific modifications of this program, itself a derivation of the fin program of the lobe-finned fish ancestral to all tetrapods (Petit et al., 2017; Pieretti et al., 2015; Shubin et al., 1997).

Limb-specific transcription factors (TFs) are important elements of the limb program: paired-like homeodomain 1 (*Pitx1*) is an HL-restricted TF gene that is expressed throughout the posterior mesoderm and consequently in the early HL bud but not in FL (Lanctôt et al., 1997; Lamonerie et al., 1996). Genetics experiments in mice suggest that Pitx1 is an important upstream regulator of HL patterning: *Pitx1*$^{-/-}$ mice develop HLs that lack several key HL characteristics (Lanctôt et al., 1999; Szeto et al., 1999). This role is conserved in evolution (Chan et al., 2010). Strikingly, *Pitx1*$^{-/-}$ HLs fail to develop the load-bearing architecture of the knee: they lack a patella and have elbow-like bone contacts between the two bones of the zeugopod and the femur, which is twisted and shortened. At the molecular level, *Pitx1*$^{-/-}$ HLs are deficient in the expression of another limb type-restricted TF gene: *Tbx4* (Lanctôt et al., 1999). Rescuing *Tbx4* expression via a *Prx1*-driven *Tbx4* transgene rescues some features lost in the *Pitx1*$^{-/-}$ HL, including femur length and certain qualitative muscle patterning characteristics (Ouimette et al., 2010).

In chick, leg and wing patterning has been correlated by various means with the expression of *Tbx4* and the closely related FL-restricted *Tbx5* (Gibson-Brown et al., 1998; Ohuchi et al., 1998; Rodriguez-Esteban et al., 1999; Takeuchi et al., 1999), but the capacity of these proteins to sufficiently determine HL versus FL morphology of the skeleton in the mouse is, however, less definitive (Ouimette et al., 2010). *Pitx1* plays a prominent role in patterning the skeleton and has the capacity to generate HL-like features in FL: ectopic expression of *Pitx1* in the FL of mice leads to structural changes in the FL skeleton, as well as ectopic expression of the HL-restricted TF *Hoxc10* (DeLaurier et al., 2006; Minguillon et al., 2005). In humans, mutations leading to ectopic *PITX1* expression in the FL cause Liebenberg syndrome, a disease in which the FLs of patients display HL-like patterning features (Spielmann et al., 2012).

The breadth and characteristics of the *Pitx1*-directed HL program are not well understood: what is the extent of *Pitx1*-dependent gene regulation and to what extent is this *Pitx1*-dependent gene regulatory network unique to the HL? Here, we use expression profiling of morphologically stage-matched FL and HL, combined with profiles of chromatin marks in these limbs, to illustrate the gene regulatory networks that drive FL and HL development. We also isolate the *Pitx1*-directed elements of the HL program through expression profiling of *Pitx1*$^{-/-}$ mice and ChIPseq of Pitx1 in E11.5 HL. We show that the programs that drive FL and HL development are very similar, marked by the expression of relatively few limb type-restricted genes. We also show that *Pitx1* largely acts upon a chromatin landscape and genetic program that are common between FL and HL. Although the chromatin landscape of select *Pitx1*-dependent genes varies in accordance with their enriched expression in HL versus FL, the *Pitx1*$^{-/-}$ phenotype is principally defined by an expression loss of genes common to both limbs. In conjunction with the loss of anterior skeletal features in the *Pitx1*$^{-/-}$ HL, we observe direct Pitx1 targeting of chondrogenic genes in the HL, suggesting that Pitx1 generates HL-specific features by targeting common limb elements involved in chondrogenic expansion during early HL development.

[1]Institut de Recherches Cliniques de Montréal, Montréal, QC, H2W 1R7 Canada. [2]Department of Experimental Medicine, McGill University, Montreal, QC, H4A 3J1 Canada. [3]Department of Biochemistry, McGill University, Montreal, QC, H3G 1Y6 Canada. [4]Department of Human Genetics, McGill University and Genome Quebec Innovation Centre, Montreal, QC, H3A 0G1 Canada.

*Author for correspondence (jacques.drouin@ircm.qc.ca)

J.D., 0000-0001-8226-5691

Received 15 May 2017; Accepted 4 August 2017

Development (2017) 144, 3325-3335 doi:10.1242/dev.154864

RESULTS

The HL and FL programs are defined by a limited number of limb type-restricted genes

In order to examine the extent of the limb-specific developmental programs, we compared the transcriptomes of morphologically stage-matched FL and HL by RNAseq analysis. Targeting an early, comparable stage of development between FL and HL, we chose to evaluate E10.5 FL and E11.0 HL, stages at which the limb bud has completely emerged from the flank but before the bud acquires any hint of a paddle-like morphology. At this stage, the anterior and posterior margins of the bud are parallel to each other and perpendicular to the flank, which corresponds to a somite count of 33-36 somites in FL and 38-42 somites in HL, stages that will henceforth be referred to as E10.5 and E11.0, respectively (Fig. 1A). Using a false discovery rate (FDR) cutoff of 0.01, we observe 986 genes that are differentially expressed between FL and HL, although the vast majority of these differences are low-magnitude expression changes, i.e. less than 2-fold changes (Fig. 1B, Fig. S1). These low-magnitude changes, however, are not biologically spurious: for example, HLs show a 27% reduction in *Gli3* expression and a corresponding 66% increase in *Shh* expression, and subtle changes in gene dosage of these anterior-posterior patterning genes have been previously associated with limb-specific morphological changes (Li et al., 2014).

We observe a relatively narrow network of genes that are expressed in a limb type-restricted manner, defined here as a $\log_2$ fold change greater than 3 (Fig. 1B,C). The extent of the FL-restricted gene network is effectively limited to *Tbx5* and the predicted gene *Gm43050*, an antisense transcript present at the *Tbx5* locus (Fig. 1C). In HL, the network of restricted genes is slightly more extensive, consisting of *Pitx1*, *Tbx4*, *Isl1*, and several of the 5′ *HoxC* genes. Much is known about these prominent genes of the limited HL-specific network: *Pitx1* and *Isl1* are genetically complementary, as both are upstream of *Tbx4*, although *Pitx1* contributes to the development of anterior HL structures while *Isl1*$^{-/-}$ mice fail to develop posterior HL elements, such as the ischium and zeugopod (Itou et al., 2012). *Hoxc10* and *Hoxc11*, in conjunction with their paralogs in the *HoxA* and *HoxD* clusters, are necessary in HL for the development of the stylopod and zeugopod, respectively (Wellik and Capecchi, 2003). *Gm53*, a long non-coding RNA located 5′ of *Hoxb9*, shows HL-restricted expression, although *Hoxb9* itself, which was previously shown to be expressed preferentially in the leg of chick (Nelson et al., 1996), plays a role with the other *Hox9* paralogs in the establishment of the posterior limb field in FL exclusively (Xu and Wellik, 2011). *Rxfp1*, a relaxin family peptide receptor gene that shows HL-restricted expression, is not known to be associated with limb patterning defects, although its ligand, relaxin, is associated with negative regulation of collagen turnover, TGFβ signaling, and fibrosis (Samuel et al., 2005). The presence of these known limb regulators in the differentially expressed dataset, although accompanied by a few novel limb type-restricted genes, validates the results of our transcriptomic approach.

The *Pitx1* gene regulatory network partially overlaps with the network of limb-enriched gene expression

With a thorough characterization of FL versus HL gene regulatory networks in hand, revealing extensive low-magnitude expression

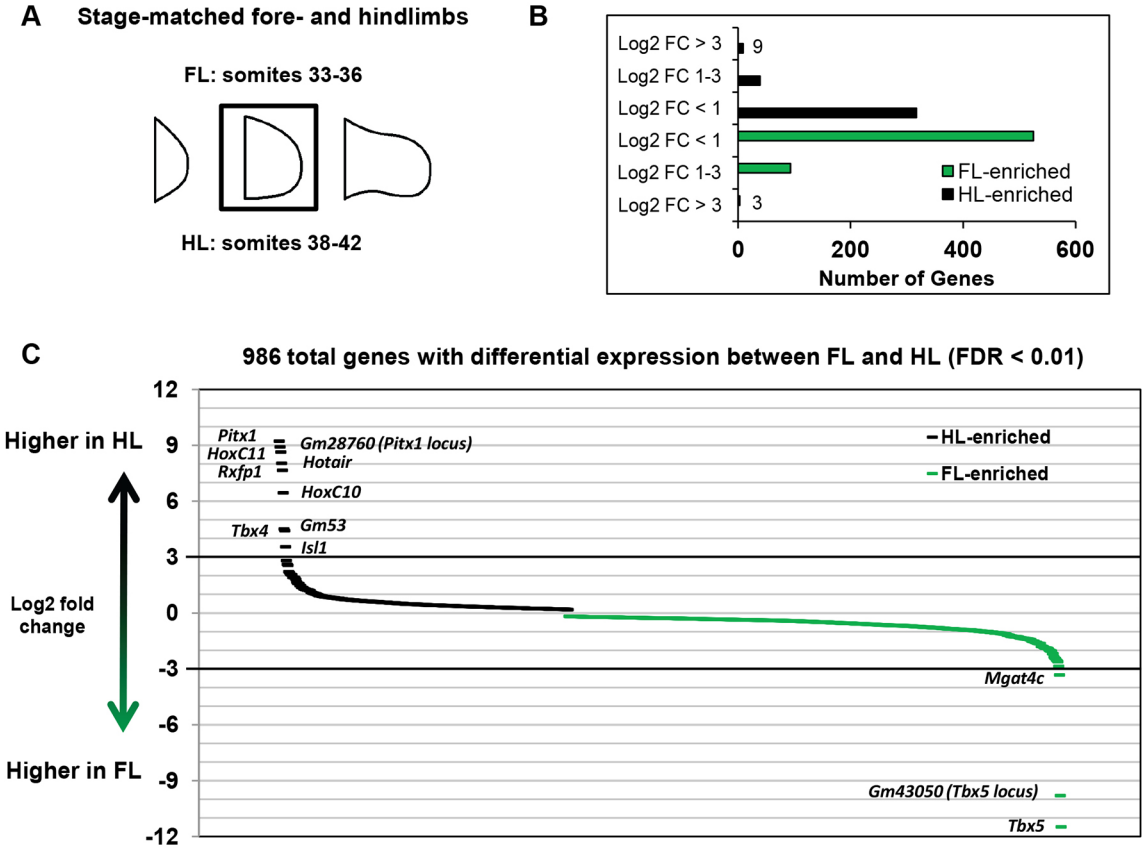

Fig. 1. Very few genes are limb type restricted in mouse embryos. (A) Representation of stage-matched FL and HL used for expression profiling by RNAseq. (B) Distribution of differentially expressed genes between FL and HL, binned according to $\log_2$ fold changes (FC). (C) Rank order by $\log_2$ fold change of all differentially expressed genes between FL and HL.

Development (2017) 144, 3325-3335 doi:10.1242/dev.154864

changes and very few limb type-restricted genes, we sought to characterize the *Pitx1* gene regulatory network at E11.0 to better understand its role in the HL program. We performed expression profiling of E11.0 *Pitx1*$^{-/-}$ versus wild-type (wt) HL and cross-compared this with our stage-matched FL versus HL expression profiling analysis (Fig. 2A). Using a conservative threshold (FDR<0.001) we identified 689 genes that are *Pitx1* dependent. Of these, most are not expressed in a limb-specific manner: 538 genes show no preference between FL and HL at FDR<0.01 (Fig. 2B). The genes that do show limb-enriched expression can be separated into four categories: *Pitx1*-dependent genes with HL-enriched expression; *Pitx1*-dependent genes with FL-enriched expression; HL-enriched genes that show increased expression in the *Pitx1*$^{-/-}$ HL; and FL-enriched genes that show increased expression in the *Pitx1*$^{-/-}$ HL. Of these groups, the set of *Pitx1*-dependent HL-enriched genes and the set of FL-enriched genes that show an increase in expression in the *Pitx1*$^{-/-}$ HL define the limb-specific components of the *Pitx1* gene regulatory network.

The set of *Pitx1*-dependent HL-enriched genes is notably marked by positive controls *Pitx1* and *Tbx4*, but in addition to these expected genes we find *Hoxa13* and several other 5′ genes of the *HoxA* cluster, including *Evx1*, *Evx1os* and *Hottip* (Fig. 2B, Table S1). Also prominently featured in this group is *E130114P18Rik*, which encodes a long non-coding RNA of unknown function; this gene shows a 4-fold preference in expression in HL, and a 4-fold decrease in HL expression in the absence of *Pitx1*. The *Pitx1*-dependent HL-enriched genes constitute the largest category with a limb-enriched expression profile, which also includes *Tgfb3*, *Gtf2ird1* and, interestingly, *Hand2*, which is important for the establishment of limb bud polarity and the onset of *Shh* expression (Galli et al., 2010).

FL-enriched genes that show an increase in expression in *Pitx1*$^{-/-}$ HL represent potential components of the limb program that are normally downregulated in the endogenous HL developmental program, where *Pitx1* is normally expressed. *Pitx2* is notably present on this list, as are several genes that are typically expressed in anterior compartments of the wt FL, including *Epha3* and *Gria2* (Fig. 2B, Table S2A). The set of genes that show HL-enriched expression as well as increased expression in the absence of *Pitx1* constitutes a small list that most prominently includes *Isl1*, a known genetic parallel of *Pitx1*, as well as the HL-specific *Rxfp1* (Table S2B). It is likely that the genes in this list are components of the *Isl1*-dependent posterior HL developmental program that persists unimpeded by the loss of *Pitx1*.

The last set of genes, showing *Pitx1*-dependent and FL-enriched expression, are a peculiar group as they represent components that are more prominently featured in the FL program that are nonetheless significantly decreased in the *Pitx1*$^{-/-}$ HL (Table S3). This group contains genes known to be involved in diverse processes, from proximal limb development and chondrogenesis to, interestingly, many genes associated with the establishment of anterior domains in anterior-posterior limb patterning. *Shox2*, an

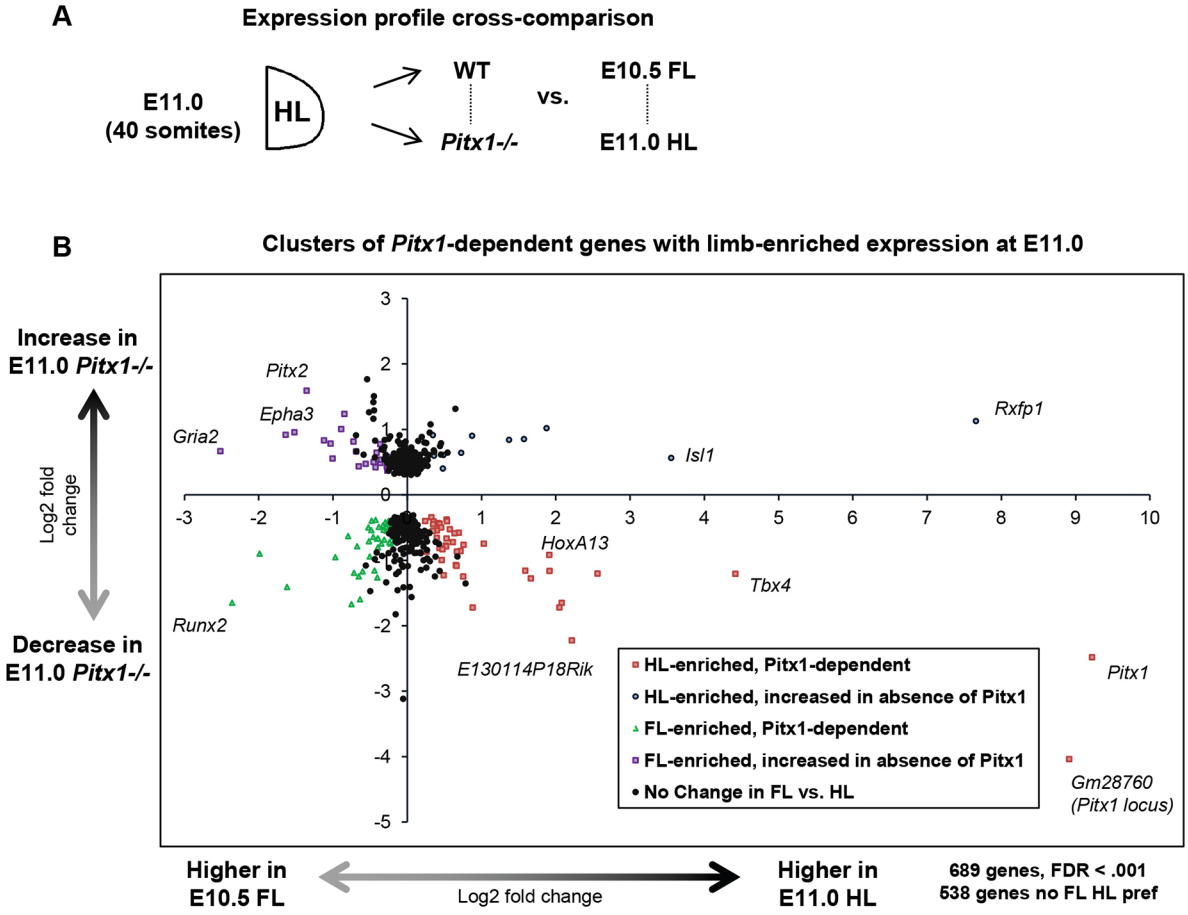

Fig. 2. Relation between limb-restricted expression and dependence on *Pitx1*. (A) Expression profiling comparisons, matching stage-matched wt FL and HL and *Pitx1*$^{-/-}$ HL analyses. (B) The $\log_2$ fold changes of gene expression in FL versus HL (*x*-axis) versus $\log_2$ fold change in E11.0 *Pitx1*$^{-/-}$ versus wt HL (*y*-axis). All genes with FDR<0.001 in the E11.0 *Pitx1*$^{-/-}$ versus wt comparison are shown.

Development (2017) 144, 3325-3335 doi:10.1242/dev.154864

important gene for proximal development of both HLs and FLs, is an upstream regulator of *Runx2* (Cobb et al., 2006); both of these genes are FL enriched and *Pitx1* dependent. *Gli3* and *Cdon*, which have an antagonistic genetic relationship with *Shh*, are also present in this set, indicating *Pitx1*-dependent expression despite the relative suppression of these genes in wt HL versus FL (Mo et al., 1997; Probst et al., 2011; Cardozo et al., 2014). Taken together, these data highlight the complex nature of the *Pitx1*-dependent gene network, as many *Pitx1*-dependent genes in these four categories have different or even opposing functions.

Pitx1 targets a limb program that is already primed for use in FL

In order to investigate the direct targets of Pitx1, we performed ChIPseq of Pitx1 in E11.5 HL. We also performed ChIPseq of the FL-restricted TF Tbx5, with the aim of using the targets of these limb-specific TFs as seeds for the investigation of limb-specific enhancer elements. In total, we isolated 10,273 peaks in our Tbx5 dataset and over 50,000 peaks in our Pitx1 dataset. For Pitx1, however, we isolated the peaks that match a corresponding ChIPseq replicate, performed using a different antibody in the same tissue (Infante et al., 2013). This corresponding dataset shows fewer total peaks, but of the 25,025 present 71% are covered by our data. This final list of 17,783 peaks thus represents a highly reliable list of Pitx1 target sites (Fig. 3A). We find that Pitx1 and Tbx5 predominantly bind gene-distant, non-promoter regions (Fig. 3B). Interestingly, the top-scoring underlying motif for Tbx5 is not a T-box half-site (TCACACCT), but a composite T-box–Hox site that contains five bases of the T-box half-site directly abutting the six core bases of a Hox binding site (Fig. 3C). Pitx1 sites are principally enriched for the canonical TAATCC Pitx1 binding site, as well as Hox and bHLH sites; unlike Tbx5, however, these Hox sites are randomly dispersed around the principal Pitx1 motif and not in a sequence-specific orientation (data not shown).

In addition to the expression profiles of stage-matched FL and HL, we also generated a library of chromatin mark data in these limbs. Using the targets of Pitx1 and Tbx5 as seeds for a screen of possible limb-specific enhancer regions, we evaluated the profiles of chromatin modifications associated with active and repressed chromatin (Fig. 3D-G), namely acetylation of lysine 27 of histone H3 (H3K27ac) and trimethylation of lysine 27 of histone H3 (H3K27me3), respectively, in stage-matched FL and HL (Cao et al., 2002; Shlyueva et al., 2014; Cotney et al., 2012). For these analyses, only Pitx1 and Tbx5 peaks at least 2.5 kb from the nearest transcription start site (TSS) were used so as to avoid contaminating our analysis with promoter regions, which have a different chromatin organization compared with enhancers. These TSS-proximal peaks represent 16% and 13% of the total, respectively. We found that the chromatin surrounding direct Pitx1 and Tbx5 targets is in largely the same state in both FL and HL (Fig. 3D-G), comprising a bimodal H3K27ac peak and a depletion of H3K27me3, an indication of enhancer chromatin in an active state. The ratio of H3K27ac signal between FL and HL is similar at sites of Pitx1 or Tbx5 binding: in fact, between limbs and comparing 100 bp bins across the entire genome, all chromatin marks that we evaluated correlate with each other very strongly, with an average Pearson's correlation coefficient of 0.94 (Fig. S1B). In light of this similarity, it is clear that Pitx1 does not globally change the epigenetic state of the limb development program, but rather acts upon genomic targets of an epigenetic state shared between FL and HL.

A small set of Pitx1 targets and Hox loci show limb-enriched chromatin profiles

Although the overall pattern of Pitx1 targets suggests a common state between limbs, there are 129 non-promoter Pitx1 targets that show a 2-fold enrichment in H3K27ac signal in the 2 kb window spanning the Pitx1 peak summit. We isolated these sites, assigned them to their putative target genes using the GREAT tool (McLean et al., 2010), and then cross-referenced this list of putative targets with our set of HL-enriched genes at FDR<0.01 (Fig. 4A). The GREAT tool associates ChIPseq peaks with nearby genes within a 5 kb to 1 Mb dynamic genomic window. The sites most enriched for H3K27ac in HL are at the truly HL-restricted genes, namely *Pitx1*, *Tbx4*, *Isl1* and the *HoxC* cluster, although several genes of the *HoxA* cluster also show HL-enriched H3K27ac at Pitx1 targets in conjunction with HL-enriched expression (Fig. 4B). This pattern corresponds with an enrichment of H3K4me3 over the 5′ side of the *HoxA* locus in HL, as well as a depletion of H3K27me3 over the same region (Fig. S2). This pattern of chromatin marks and HL-enriched gene expression is also apparent at the *HoxD* locus (Fig. S3). To varying extents, all Hox loci show a preference for HL expression in the 5′ side of the cluster and a corresponding preference for FL expression in the 3′ side of the cluster, although the boundaries at which expression becomes FL-enriched or HL-enriched vary by cluster (Figs S2-S5).

Of these HL-enriched genes near Pitx1 sites that show HL-enriched H3K27ac signal, only half are *Pitx1* dependent. Pitx1 sites near *Col5a1*, *Hoxc10* and *Hand2* are shown as representative loci (Fig. 4C). Interestingly, in light of the fact that Pitx1 has been shown to be present at and drive *Hoxc10* and *Hoxc11* expression (Infante et al., 2013; Park et al., 2014; DeLaurier et al., 2006), *Hoxc10* shows only a limited degree of *Pitx1* dependence, with a 25% reduction in expression at E11.0 in $Pitx1^{-/-}$ HL (FDR=0.006), while *Hoxc11* is not *Pitx1* dependent at E11.0 and the expression of neither gene is *Pitx1* dependent at E11.5 (Fig. 4B, Fig. S5A). These results reveal putative enhancers where Pitx1 action may increase active chromatin marks, but also highlight the complementary, interrelated nature of the HL-restricted gene network.

Pitx1 directly targets *Sox9* and regulates the chondrogenic program in HL

In an effort to isolate the most certain and direct targets of Pitx1, we sought to find genes with *Pitx1*-dependent expression in HL at both E11.0 and E11.5 at a highly significant threshold, and then to focus on these differentially expressed genes that show evidence of Pitx1 binding within the associated locus. We used two strategies to correlate Pitx1 binding sites with target genes: published 4C contacts data, at loci for which it is available (Andrey et al., 2017), as well as the aforementioned GREAT tool. Using FDR<0.00001 in both the E11.0 and E11.5 $Pitx1^{-/-}$ expression profiles reveals 67 genes, the overwhelming majority of which show decreased expression in $Pitx1^{-/-}$: 54 genes are downregulated, whereas only 13 genes show increased expression in the $Pitx1^{-/-}$ HL (Fig. 5). The top four Pitx1-dependent genes most frequently targeted by Pitx1 at regions of established enhancer-promoter contact are *Sox9*, *Tcf7l2*, *Tbx15* and *Tbx18* (Fig. S1C): Pitx1 is found at a total of 41 regions that contact these genes (Fig. 5).

To assess the dynamic gene expression changes over the course of development, we also isolated the set of genes that are differentially expressed in the $Pitx1^{-/-}$ HL at E11.5 that show no differential expression at E11.0 (Fig. 6A). We found that twice as many genes show decreased versus increased expression in the $Pitx1^{-/-}$ HL: 220 versus 102, respectively (Fig. 6A). Gene

Development (2017) 144, 3325-3335 doi:10.1242/dev.154864

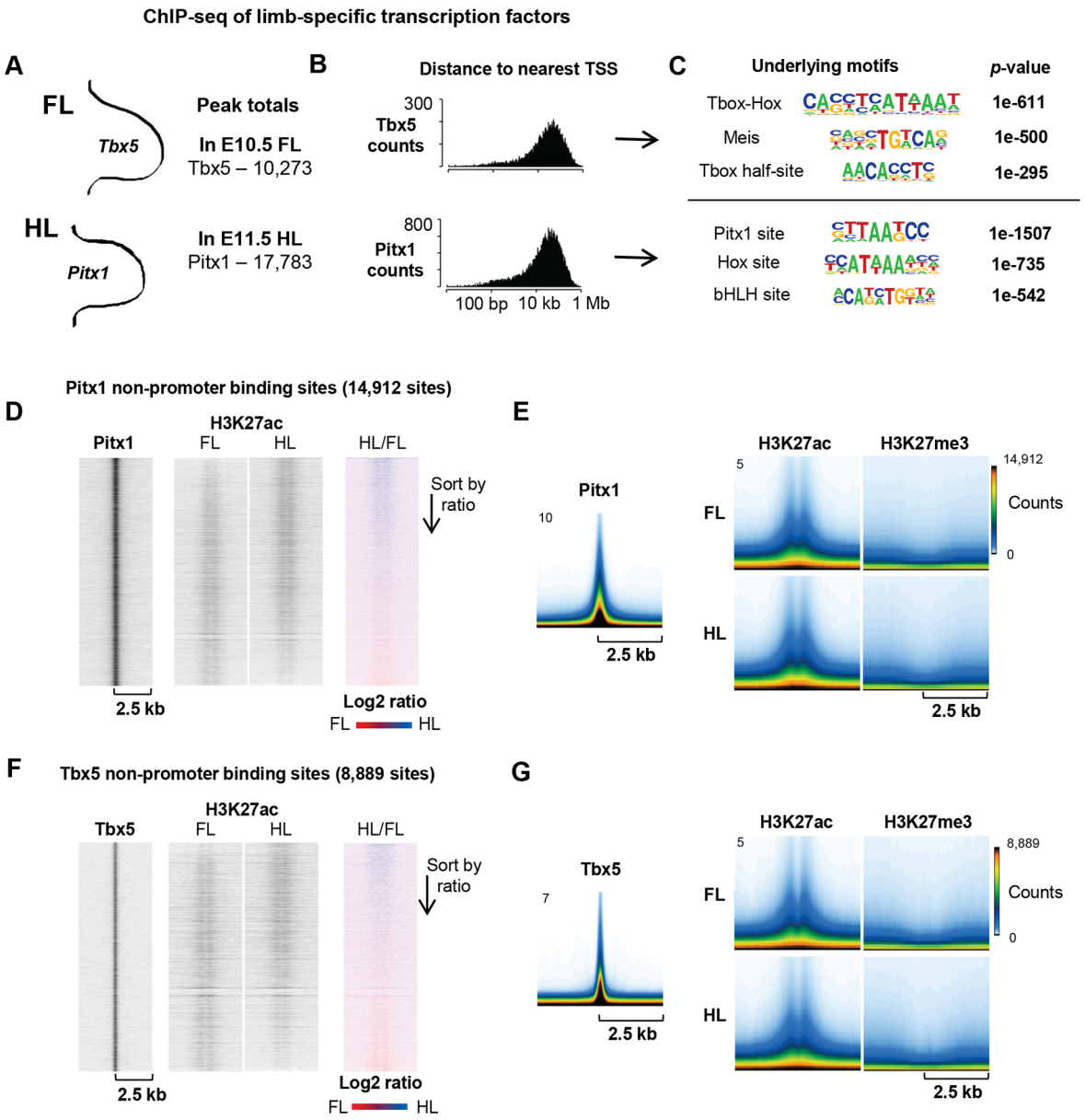

Fig. 3. Conserved epigenetic landscape at putative enhancer loci in FL and HL. (A) Total number of peaks in Tbx5 and Pitx1 ChIPseq, performed in E10.5 FL and E11.5 HL, respectively. (B) Histogram of all Tbx5 and Pitx1 peaks, binned by peak distance to the TSS of the nearest gene. Up to one megabase, distance to the TSS is divided into 200 bins and set to a $\log_{10}$ scale. (C) *De novo* motif search results, ordered by *P*-value, for Tbx5 and Pitx1 ChIPseq peaks. (D,F) Heatmaps of ChIPseq signal at Pitx1 non-promoter sites, i.e. at least 2.5 kb from the nearest TSS. Each heatmap covers a 5 kb window, charting the tag intensity of Pitx1 (D) and Tbx5 (F) along with the H3K27ac signal in stage-matched FL and HL, followed by the ratio of HL/FL tags. Each heatmap is sorted in the order of the HL/FL H3K27ac ratio. (E,G) Condensed profiles of ChIPseq signals for Pitx1 (E) and Tbx5 (G), as well as the H3K27ac and H3K27me3 profiles in FL and HL. The condensed profiles are merged views of the chromatin profiles surrounding every ChIPseq peak. The *y*-axis indicates the normalized signal of the ChIPseq data, while the color scale corresponds to how many TF binding sites have a chromatin profile of the indicated intensity.

Ontology analysis shows that this larger set of *Pitx1*-dependent genes is enriched for genes associated with proteinaceous extracellular matrix, as well as collagens; in other words, genes associated with chondrogenesis and other tissues such as tendons, ligaments and muscle connective tissue (Fig. 6B).

We assayed the expression pattern of *Sox9* in E11.5 wt and *Pitx1*$^{-/-}$ HL by *in situ* hybridization in order to assess the spatial changes in expression that correspond to the quantitative changes we observe in our E11.0 and E11.5 expression profiles. We see a prominent patch of *Sox9* expression in the anterior proximal wt HL that is absent in the *Pitx1*$^{-/-}$ HL (Fig. 7A). We also tracked the skeletal phenotype of wt and *Pitx1*$^{-/-}$ HL, as well as wt FL, over the course of their development from E12.5 to E14.5, staining for cartilage with Alcian Blue 8GX (Fig. 7B). We see that this anterior patch of *Sox9* expression corresponds to regions of the HL that develop into the robust elements of the distal femur and proximal tibia, corresponding to the regions most affected in the *Pitx1*$^{-/-}$ HL. This large anterior condensation never forms in the *Pitx1*$^{-/-}$, and a weak pattern of condensation patterned in the basic Y-shape of the FL still lacks intensity relative to the FL skeletal phenotype (Fig. 7B). These condensations are thin and undeveloped at E13.5, and by E14.5 there is a visible kink in the developing femur of the *Pitx1*$^{-/-}$ HL, a contrast to the patch of cells that migrate down from the shoulder to form the deltoid tuberosity in the humerus (Blitz et al., 2013), and an

Development (2017) 144, 3325-3335 doi:10.1242/dev.154864

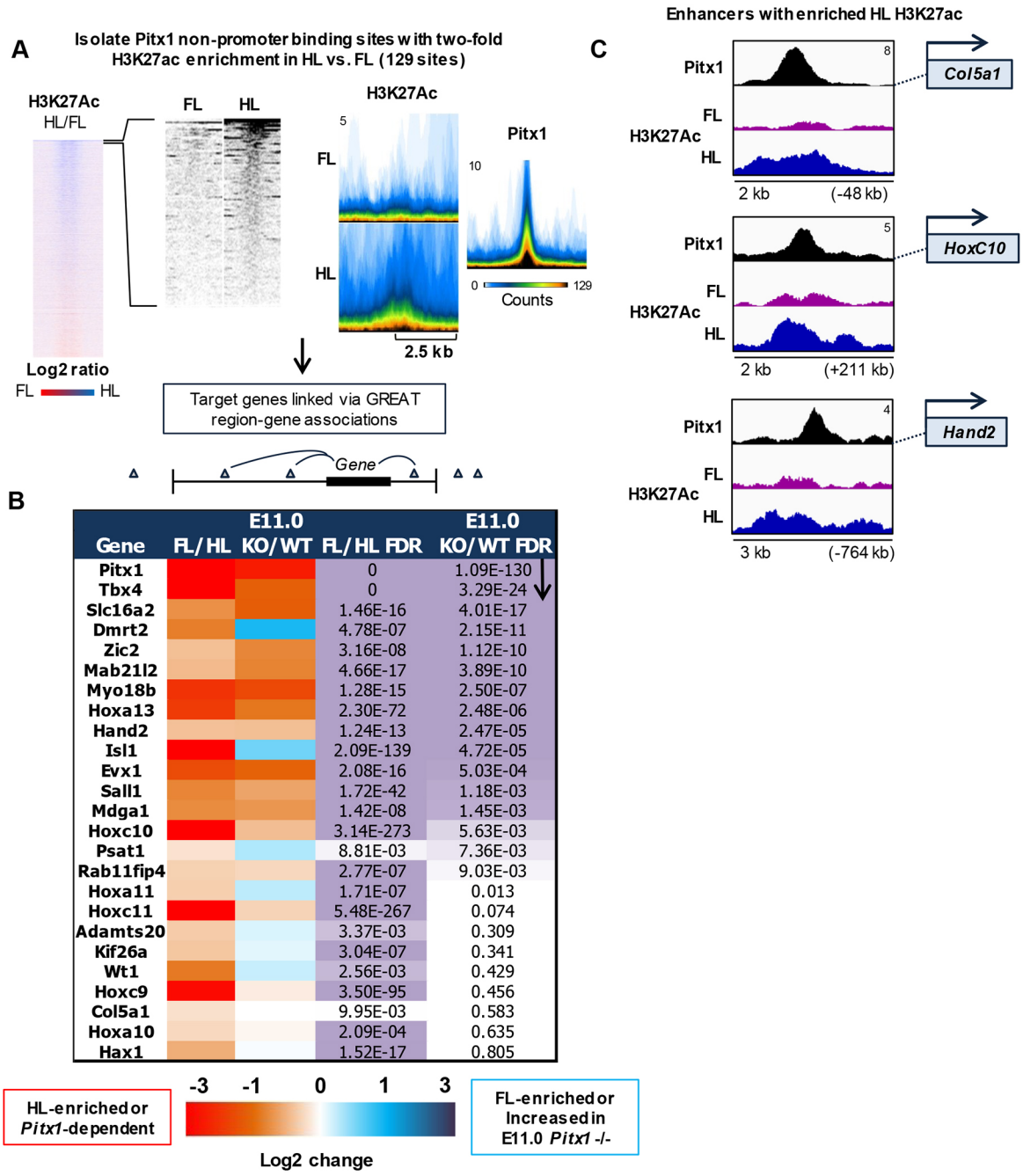

Fig. 4. Active epigenetic marks are enriched at limb-specific loci. (A) Heatmaps and condensed profiles of the H3K27ac signal in FL and HL for the 129 Pitx1 non-promoter sites that show a ratio of HL/FL signal greater than 2. The condensed profile of Pitx1 at these sites is also shown. (B) Pitx1-targeted genes that show HL-enriched expression at FDR<0.01, along with the degree of *Pitx1* dependence of these associated genes. The $\log_2$ fold change of gene expression is shown by heatmap for the stage-matched FL versus HL, as well as E11.0 *Pitx1*$^{-/-}$ (KO) versus wt HL comparisons. The chart is sorted by the FDR of differential gene expression in the E11.0 *Pitx1*$^{-/-}$ versus wt comparison. (C) Three Pitx1-bound loci showing a 2-fold enrichment of H3K27ac in HL relative to FL.

indication that the early chondrogenic defects observed in the *Pitx1*$^{-/-}$ result ultimately in failed long-bone formation in the stylopod. Pitx1 direct targeting of *Sox9* (Fig. 7C) and related chondrogenic genes at earlier stages of limb development might thus be responsible for the many skeletal defects observed in the *Pitx1*$^{-/-}$ HL at later stages.

DISCUSSION

The FL and HL of tetrapods evolved from the pectoral and pelvic fins, respectively, during the fin-to-limb transition 360 million years ago (reviewed by Clack, 2009). The role of *Pitx1* in generating differences between posterior and anterior appendages has far-reaching evolutionary implications and is not unique to tetrapod limbs: the expression of *Pitx1* has been associated with the presence or absence of pelvic fins in species of stickleback, which are ray-finned fish with distinct ancestry relative to the lobe-finned predecessors of modern tetrapods (Chan et al., 2010). Recent studies suggest that, between species, the early-stage limb development program is robustly conserved between divergent mammalian species (Sears et al., 2015). The classical model follows that FLs and HLs are serial homologs, although recently an alternative hypothesis has been put

Development (2017) 144, 3325-3335 doi:10.1242/dev.154864

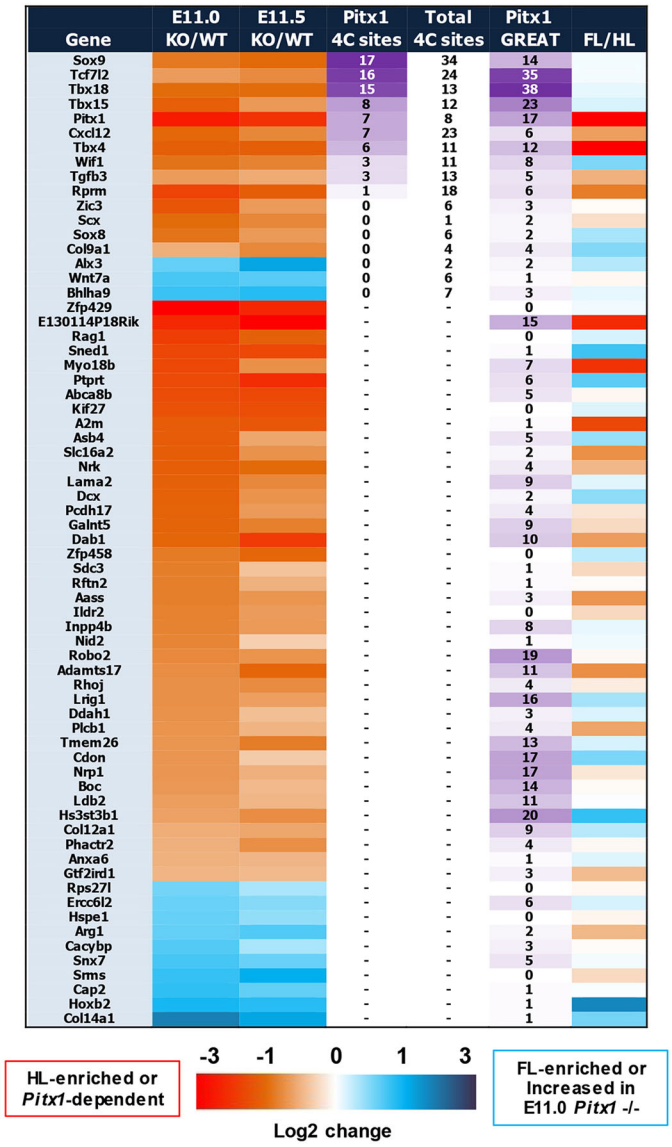

Fig. 5. Cross-stage analysis of *Pitx1*-dependent genes linked to genomic landscape. *Pitx1*-dependent genes that show highly significant changes at both E11.0 and E11.5, using FDR<0.00001 for both comparisons. The $\log_2$ fold change of gene expression is shown by heatmap at both stages, as well as for stage-matched FL versus HL (last column). The total number of 4C sites (Andrey et al., 2017) and the number of Pitx1 binding sites present in these 4C contact regions are indicated for each gene. The number of Pitx1 binding sites that occur within the GREAT-defined window of region-gene associations is also shown for each gene.

forth that the extensive similarities between FLs and HLs are the result of convergent evolution during the fin-to-limb transition. Regardless of the origin of the similarity between the developmental programs of FLs and HLs, however, it is clear that the responsibility of generating limb-specific features of the FL and HL programs rests with a narrow network of limb-specific elements of this program. Our results match these evolutionary constraints, with few limb type-restricted genes and a broadly conserved developmental program.

HL patterning is largely implemented by transcriptional, not epigenetic, actions

Pitx1, a prominent HL-restricted gene, can manifest its role in HL patterning by tinkering with the established and common limb program or by directly effecting skeletal pattern by regulation of the amount, timing and placement of chondrogenic condensation during limb development. It is clear, in light of our results and the abundance of data across species, that there is not an extensive, limb type-restricted network downstream of *Pitx1*. Our results indicate that Pitx1 binds to developmental enhancers that are ready to use in FL, which is to say that Pitx1 does not appear to engage in extensive remodeling of the chromatin state of its targets. This common state between FL and HL suggests that Pitx1 acts by direct transcriptional regulation rather than chromatin remodeling. The fact that the preponderance of genes misregulated in the *Pitx1*$^{-/-}$ HL are downregulated, as opposed to derepressed in its absence, combined with the active chromatin profile around Pitx1 target sites, suggests that Pitx1 predominantly functions to activate its transcriptional targets. Finally, the fact that Pitx1 targets a region with an HL-enriched chromatin profile near the *Pitx1* gene itself might suggest autoregulation and, indeed, positive autoregulation of *Pitx1* expression has been shown in the pituitary (Goodyer et al., 2003).

Transcriptional activation is usually accompanied by enhancement of active enhancer chromatin marks, but this is different from an action such as that of pioneer factors which instill chromatin accessibility where there was none. Our data do not support a significant pioneer role for Pitx1. Rather, the data indicate that Pitx1 acts as a classical TF at enhancers in an active chromatin state (Fig. 7D).

Pitx1 modifies the common limb program as a member of a narrow HL-specific network

Previous analyses suggest a limited overlap between the HL-specific components of the HL program: *Isl1* partially drives *Tbx4* expression early in limb development, but is not necessary for *Tbx4* expression upon HL bud outgrowth, nor is it required for *Pitx1* or *Hoxc10* expression (Itou et al., 2012; Kawakami et al., 2011). Our analysis confirms the parallel and independent nature of *Pitx1* and *Isl1*, as *Isl1* expression is even increased in the absence of *Pitx1*. The prominent target of *Isl1*, however, which is known to be *Hand2* (Itou et al., 2012), is shown here at E11.0 to be *Pitx1*-dependent. We do not see the complete abrogation of *Shh* expression in the *Pitx1*$^{-/-}$ HL, however, as is the case in *Hand2*$^{-/-}$ HL (Galli et al., 2010) and *Isl1*$^{-/-}$ HL (Itou et al., 2012), although there is a 40% reduction in *Shh* expression in the E11.0 *Pitx1*$^{-/-}$ HL (FDR=0.007). These results further complement transgenic experiments in which ectopic *Pitx1* expression in the FL suppresses *Shh* signaling pathways and posteriorly expands the territory of *Gli3* expression (DeLaurier et al., 2006).

At the same time, *Pitx1* regulates components of the anterior patterning program, including *Gli3*, which are disrupted in the absence of *Pitx1*. Although much of the research on *Shh* and *Gli3* focuses on digit patterning in the autopod, it was shown that *Gli3*$^{-/-}$ HLs display a reduction in femur size (Litingtung et al., 2002). The decrease in femur length in the *Pitx1*$^{-/-}$ might in part be due to the decreased expression of *Gli3* in these HLs. In related work, *Irx3* and *Irx5* were shown to have HL-specific contributions to anterior limb pattern in a manner that is dependent on the interplay between *Shh* signaling and anterior patterning genes such as *Gli3* (Li et al., 2014). *Irx5* is not differentially expressed in *Pitx1*$^{-/-}$ HL at E11.0 or E11.5, however, and *Irx3* shows only a slight decrease in expression in *Pitx1*$^{-/-}$ HL above the threshold of significance taken here (FDR=0.014). It is therefore likely that *Pitx1* and *Irx3/5* both contribute to the development of anterior structures in HL, but not interdependently.

Tbx15 and *Tbx18* are revealed in this study as direct targets of Pitx1, with Pitx1-dependent expression in the HL, although both

Development (2017) 144, 3325-3335 doi:10.1242/dev.154864

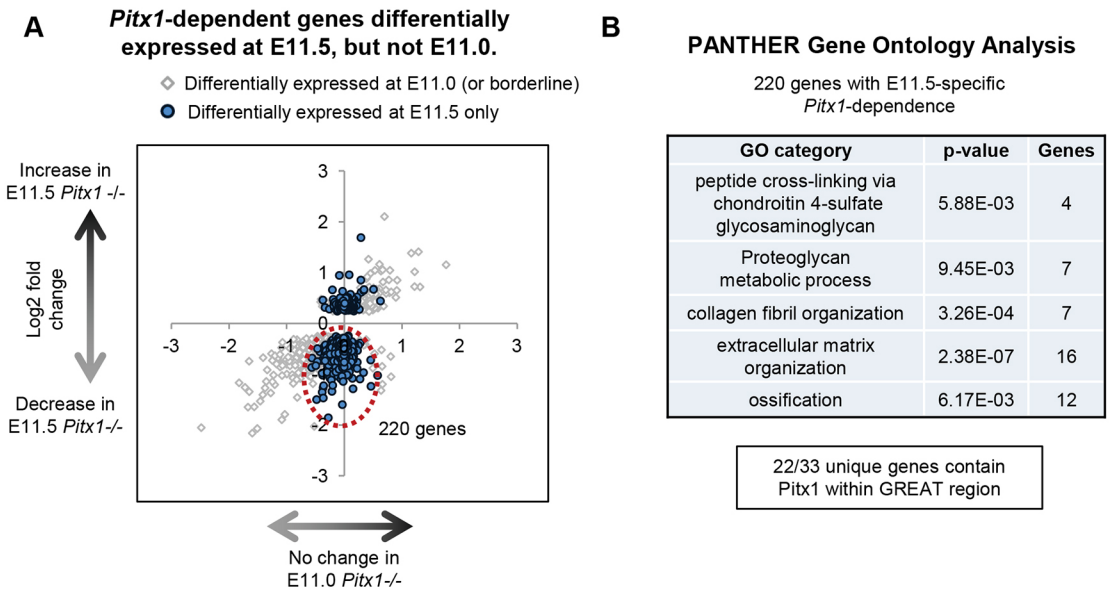

Fig. 6. Identification of HL stage-specific *Pitx1*-dependent genes. (A) Two-dimensional representation of genes showing *Pitx1*-dependent gene expression at E11.5 but not at E11.0. The *x*-axis indicates the $\log_2$ fold change of gene expression in the E11.0 *Pitx1*$^{-/-}$ versus wt HL, while the *y*-axis indicates the $\log_2$ fold change of gene expression in the E11.5 *Pitx1*$^{-/-}$ versus wt HL. The genes in blue show no significant change in expression at E11.0 (FDR>0.1) but show highly significant changes at E11.5 (FDR<0.001). Genes in gray have a FDR<0.1 at E11.0. (B) The newly misexpressed genes encircled in red in A were isolated and submitted for PANTHER-sourced GO analysis, sorted by hierarchy, i.e. from the most specific GO subcategory to the most general.

genes are also expressed in the FL. *Tbx15* and *Tbx18* are closely related members of the *Tbx1* subfamily of T-box genes (Papaioannou, 2014). *Tbx15* is strongly expressed in the core mesenchyme of the developing limb bud and *Tbx15*$^{-/-}$ mice show skeletal defects in both FL and HL, including reduced femur size (Singh et al., 2005). *Tbx18* is expressed in the anterior-proximal limb mesenchyme (Kraus et al., 2001), although there are no morphological effects on the limb in *Tbx18*$^{-/-}$ mice (Bussen et al., 2004). In light of the fact that *Pitx1* is necessary for the expression of *Tbx4*, *Tbx15* and *Tbx18*, it is possible that there is a degree of functional redundancy between these genes, and that Pitx1 exerts an influence in the early HL mesenchyme by coordinating the expression of all three genes.

Our data also show that *Pitx1* directly targets *Sox9* (Fig. 7D), and there is a marked loss of *Sox9* expression in the early *Pitx1*$^{-/-}$ HL in regions that correspond to the most prominent skeletal defects in the fully formed *Pitx1*$^{-/-}$ HL. Ultimately, bones do form in the *Pitx1*$^{-/-}$ HL, so the chondrogenic cascade is not completely disrupted and *Pitx1* is not explicitly necessary for condensation and skeletogenesis in the HL. This does not preclude a role of *Pitx1* expression in directly controlling the total number of cells that condense in the anterior HL. Pitx1 might alter the rate of proliferation of uncommitted mesenchymal progenitors, directly stimulate commitment to the *Sox9*-positive chondrogenic lineage, influence proliferation of *Sox9*-positive cells, or any combination of these possibilities. This direct manner of regulation might occur complementarily to, or in concert with, Pitx1-dependent regulation of T-box family genes and anterior-posterior patterning genes. Further, expression of these regulators in the early HL bud (Marcil et al., 2003) is consistent with the present interpretation.

How to make a different limb

In summary, the broad set of Pitx1 targets suggests a role as a major modulator of the limb development program. This action is implemented through transcriptional regulation (primarily activation) of a large set of target genes. These target genes are for the most part expressed in both FL and HL and therefore the effect of Pitx1 action (and of the downstream Tbx4, or of Tbx5 in FL) is to reorganize the gene expression patterns throughout the developing bud. It is this reorganized program – the sum of small changes that create a distinction in aggregate – that defines HL identity.

MATERIALS AND METHODS

Chromatin immunoprecipitation (ChIP)

All animal experimentation was approved by the IRCM Animal Ethics Review Board and followed Canadian guidelines. ChIP was performed using limb bud tissue collected from CD1 mice ordered from Charles River Laboratories or bred in the animal facilities of the IRCM. Embryonic day (E) 0.5 was designated to be noon of the day on which a plug was found. Pitx1 ChIPseq was performed with HL tissue from mice staged at E11.5, while Tbx5 ChIPseq was performed on the FL of mice staged at E10.5. Limb buds were collected in cold 1× PBS, cross-linked with 1% formaldehyde for 14 min, and chromatin was sheared using a manual sonication probe. Previously validated homemade rabbit antibodies against Pitx1 (Lamonerie et al., 1996; Tremblay et al., 1998; Marcil et al., 2003) and Tbx5 (Georges et al., 2008) were used, and all ChIPs were performed with equal amounts of Protein A and Protein G Dynabeads (Invitrogen). These TF ChIPseq samples were sequenced on an Illumina HiSeq 4000 platform, yielding 50 bp, paired-end reads, which were then mapped to mm10 using Bowtie2 version 2.2.6 (Langmead et al., 2009). Peaks were called using MACS2 with default parameters for paired-end reads (Zhang et al., 2008), and peaks with summits present in genome-wide RepeatMasker or an Encode-sourced comprehensive empirical blacklist of regions with artificially high signal were removed, as were summits whose loci contained anomalous input signal (RepeatMasker Open-3.0, http://www.repeatmasker.org) (ENCODE Project Consortium, 2012). Pitx1 summits from our data that appeared at any region within a peak defined in Infante et al. (2013) were considered to be present in both datasets. *De novo* motif searches were performed on peaklists using HOMER with default parameters (Heinz et al., 2010). Non-promoter sites are defined as summits greater than 2.5 kb from the nearest TSS present in the gene annotation from Encode version M11 (Ensembl 86). ChIPseq tracks for visualization were created in HOMER and displayed using Integrated Genome Viewer (IGV) (Thorvaldsdottir et al., 2013).

For the chromatin profiles of stage-matched FL and HL, samples were sequenced on the Illumina HiSeq 4000 platform, yielding 50 bp, single-end

Development (2017) 144, 3325-3335 doi:10.1242/dev.154864

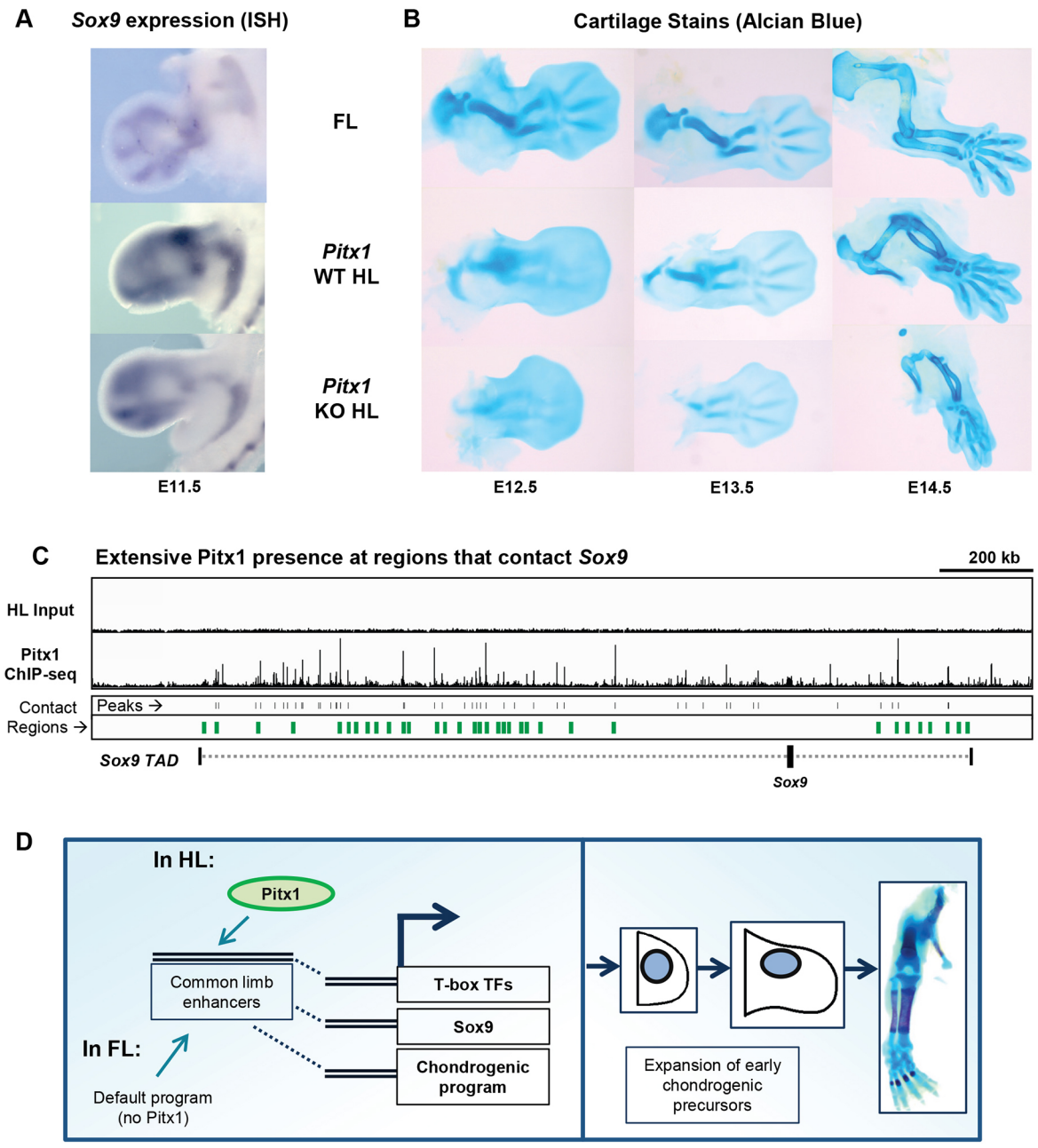

Fig. 7. Chondrogenesis is regulated by Pitx1. (A) *Sox9* expression, detected by *in situ* hybridization at E11.5 in FL, wt HL and *Pitx1*$^{-/-}$ HL. (B) Alcian Blue cartilage staining in FL, wt HL and *Pitx1*$^{-/-}$ HL. (C) ChIPseq tracks of Pitx1, HL input (control), as well as Pitx1 peak-calling hits and 4C contact regions (Andrey et al., 2017) in the 2 Mb region surrounding the *Sox9* gene. The *Sox9* TAD (Franke et al., 2016) is indicated. (D) Model of Pitx1 role in HL program. For implementation of HL identity, Pitx1 targets limb enhancers that are in a similar active chromatin state in both FL and HL. The chondrogenic program is a major target of Pitx1 action.

reads. These single-end read datasets were mapped to mm10 using Bowtie version 1.1.2 (Langmead et al., 2009). Genome-wide correlations were performed using EASeq (Lerdrup et al., 2016). Heatmaps, computed over a 5 kb window divided into 500 10-bp bins, as well as corresponding fillplots, were also created in EAseq.

Expression profiling by RNAseq

For stage-matched E10.5 FL versus E11.0 HL comparisons, limb tissue was collected from wt CD1 mice. Somites were counted for each embryo: 33-36 somite FLs were taken as E10.5 FLs and 38-42 somite HLs were taken as E11.0 HLs. Both E11.0 and E11.5 *Pitx1*$^{-/-}$ versus wt HL comparisons were performed in a Balb/c background. All animal experimentation was approved by the IRCM Animal Ethics Review Board and followed Canadian guidelines.

RNA samples were collected via silica gel spin-column purification. For E10.5 FL versus E11.0 HL, one replicate was prepared using a strand-specific ribosomal RNA-depleted RNAseq kit from Illumina (TruSeq Stranded Total RNA). One replicate of E11.0 *Pitx1*$^{-/-}$ versus wt HL was prepared using only the left HL, using a strand-specific ribosomal RNA-depleted KAPA kit (KAPA Stranded RNA-Seq Library) with Ribozero Gold (Epicentre), and one replicate of E11.5 *Pitx1*$^{-/-}$ versus wt HL was prepared using an unstranded, TruSeq mRNA enrichment library prep kit (Illumina). Two additional replicates of E10.5 FL versus E11.0 HL and E11.0 *Pitx1*$^{-/-}$ versus wt HL were prepared using the strand-specific ribosomal RNA-depleted KAPA kit with Ribozero Gold (Epicentre), and two additional replicates of E11.5 *Pitx1*$^{-/-}$ versus wt HL were prepared using an mRNA-enrichment kit

Development (2017) 144, 3325-3335 doi:10.1242/dev.154864

from NEB [NEBnext poly(A) mRNA magnetic isolation] and the KAPA Stranded RNA-Seq Library.

For each comparison, three total replicates were fused for an experimental design with two conditions and two batches for each condition. All reads were mapped to the genome using STAR (Dobin et al., 2013). Transcript features were counted using featureCounts (Liao et al., 2014). All RNAseq experiments were analyzed using edgeR with robust dispersion estimates, likelihood ratio testing, and a generalized linear model (GLM), allowing us to accommodate batch effects between replicates (Robinson et al., 2010; McCarthy et al., 2012; Zhou et al., 2014).

In situ hybridization and cartilage stains

In situ hybridization was performed using anti-digoxigenin and probes generated from *Sox9* cDNA plasmid digested with *Bam*HI. Cartilage stains of E12.5 through E14.5 mouse embryos were performed by fixing embryos in Bouin's fluid, bleaching embryos in 70% ethanol/0.1% ammonium hydroxide, staining with 0.05% Alcian Blue 8GX in 5% acetic acid, and clearing embryos with 2:1 benzyl benzoate:benzyl alcohol solution, similar to Nagy et al. (2009).

Acknowledgements

We thank Isabelle Brisson, Dimitar Dimitrov and Sara Demontigny for their work in the IRCM animal care facility; Amandine Bemmo for helpful assistance with bioinformatics analyses; Mona Nemer, University of Ottawa, for the gift of Tbx5 antibody; and Évelyne Joyal and Tabasum Abdul-Rasul for secretarial work.

Competing interests

The authors declare no competing or financial interests.

Author contributions

Conceptualization: S.N., J.D.; Methodology: S.N., J.D.; Formal analysis: S.N.; Investigation: S.N., M.L., A.H.S.; Resources: T.P., J.D.; Data curation: S.N., D.J.; Writing - original draft: S.N.; Writing - review & editing: S.N., J.D.; Visualization: S.N.; Supervision: J.D.; Project administration: J.D.; Funding acquisition: T.P., J.D.

Funding

This work was supported by grants (MOP-123213, CEEHRC EP1-120608) from the Canadian Institutes of Health Research (CIHR).

Data availability

ChIPseq and RNAseq data have been deposited at Gene Expression Omnibus under accession number GSE100734.

Supplementary information

Supplementary information available online at
http://dev.biologists.org/lookup/doi/10.1242/dev.154864.supplemental

References

Andrey, G., Schöpflin, R., Jerković, I., Heinrich, V., Ibrahim, D. M., Paliou, C., Hochradel, M., Timmermann, B., Haas, S., Vingron, M. et al. (2017). Characterization of hundreds of regulatory landscapes in developing limbs reveals two regimes of chromatin folding. *Genome Res.* **27**, 223-233.

Blitz, E., Sharir, A., Akiyama, H. and Zelzer, E. (2013). Tendon-bone attachment unit is formed modularly by a distinct pool of Scx- and Sox9-positive progenitors. *Development* **140**, 2680-2690.

Bussen, M., Petry, M., Schuster-Gossler, K., Leitges, M., Gossler, A. and Kispert, A. (2004). The T-box transcription factor Tbx18 maintains the separation of anterior and posterior somite compartments. *Genes Dev.* **18**, 1209-1221.

Cao, R., Wang, L., Wang, H., Xia, L., Erdjument-Bromage, H., Tempst, P., Jones, R. S. and Zhang, Y. (2002). Role of histone H3 lysine 27 methylation in Polycomb-group silencing. *Science* **298**, 1039-1043.

Cardozo, M. J., Sánchez-Arrones, L., Sandonis, A., Sánchez-Camacho, C., Gestri, G., Wilson, S. W., Guerrero, I. and Bovolenta, P. (2014). Cdon acts as a Hedgehog decoy receptor during proximal-distal patterning of the optic vesicle. *Nat. Commun.* **5**, 4272.

Chan, Y. F., Marks, M. E., Jones, F. C., Villarreal, G., Jr, Shapiro, M. D., Brady, S. D., Southwick, A. M., Absher, D. M., Grimwood, J., Schmutz, J. et al. (2010). Adaptive evolution of pelvic reduction in sticklebacks by recurrent deletion of a Pitx1 enhancer. *Science* **327**, 302-305.

Clack, J.-A. (2009). The fin to limb transition: new data, interpretations, and hypotheses from paleontology and developmental biology. *Annu. Rev. Earth Planet. Sci.* **37**, 163.

Cobb, J., Dierich, A., Huss-Garcia, Y. and Duboule, D. (2006). A mouse model for human short-stature syndromes identifies Shox2 as an upstream regulator of Runx2 during long-bone development. *Proc. Natl. Acad. Sci. USA* **103**, 4511-4515.

Cotney, J., Leng, J., Oh, S., Demare, L. E., Reilly, S. K., Gerstein, M. B. and Noonan, J. P. (2012). Chromatin state signatures associated with tissue-specific gene expression and enhancer activity in the embryonic limb. *Genome Res.* **22**, 1069-1080.

DeLaurier, A., Schweitzer, R. and Logan, M. (2006). Pitx1 determines the morphology of muscle, tendon, and bones of the hindlimb. *Dev. Biol.* **299**, 22-34.

Dobin, A., Davis, C. A., Schlesinger, F., Drenkow, J., Zaleski, C., Jha, S., Batut, P., Chaisson, M. and Gingeras, T. R. (2013). STAR: ultrafast universal RNA-seq aligner. *Bioinformatics* **29**, 15-21.

ENCODE Project Consortium (2012). An integrated encyclopedia of DNA elements in the human genome. *Nature* **489**, 57-74.

Franke, M., Ibrahim, D. M., Andrey, G., Schwarzer, W., Heinrich, V., Schopflin, R., Kraft, K., Kempfer, R., Jerkovic, I., Chan, W. L. et al. (2016). Formation of new chromatin domains determines pathogenicity of genomic duplications. *Nature* **538**, 265-269.

Galli, A., Robay, D., Osterwalder, M., Bao, X., Bénazet, J.-D., Tariq, M., Paro, R., Mackem, S. and Zeller, R. (2010). Distinct roles of Hand2 in initiating polarity and posterior Shh expression during the onset of mouse limb bud development. *PLoS Genet.* **6**, e1000901.

Georges, R., Nemer, G., Morin, M., Lefebvre, C. and Nemer, M. (2008). Distinct expression and function of alternatively spliced Tbx5 isoforms in cell growth and differentiation. *Mol. Cell. Biol.* **28**, 4052-4067.

Gibson-Brown, J. J., Agulnik, S. I., Silver, L. M., Niswander, L. and Papaioannou, V. E. (1998). Involvement of T-box genes Tbx2-Tbx5 in vertebrate limb specification and development. *Development* **125**, 2499-2509.

Goodyer, C. G., Tremblay, J. J., Paradis, F. W., Marcil, A., Lanctôt, C., Gauthier, Y. and Drouin, J. (2003). Pitx1 *in vivo* promoter activity and mechanisms of positive autoregulation. *Neuroendocrinol.* **78**, 129-137.

Heinz, S., Benner, C., Spann, N., Bertolino, E., Lin, Y. C., Laslo, P., Cheng, J. X., Murre, C., Singh, H. and Glass, C. K. (2010). Simple combinations of lineage-determining transcription factors prime cis-regulatory elements required for macrophage and B cell identities. *Mol. Cell* **38**, 576-589.

Infante, C. R., Park, S., Mihala, A. G., Kingsley, D. M. and Menke, D. B. (2013). Pitx1 broadly associates with limb enhancers and is enriched on hindlimb cis-regulatory elements. *Dev. Biol.* **374**, 234-244.

Itou, J., Kawakami, H., Quach, T., Osterwalder, M., Evans, S. M., Zeller, R. and Kawakami, Y. (2012). Islet1 regulates establishment of the posterior hindlimb field upstream of the Hand2-Shh morphoregulatory gene network in mouse embryos. *Development* **139**, 1620-1629.

Kawakami, Y., Marti, M., Kawakami, H., Itou, J., Quach, T., Johnson, A., Sahara, S., O'leary, D. D. M., Nakagawa, Y., Lewandoski, M. et al. (2011). Islet1-mediated activation of the beta-catenin pathway is necessary for hindlimb initiation in mice. *Development* **138**, 4465-4473.

Kraus, F., Haenig, B. and Kispert, A. (2001). Cloning and expression analysis of the mouse T-box gene Tbx18. *Mech. Dev.* **100**, 83-86.

Lamonerie, T., Tremblay, J. J., Lanctôt, C., Therrien, M., Gauthier, Y. and Drouin, J. (1996). PTX1, a *bicoid*-related homeo box transcription factor involved in transcription of pro-opiomelanocortin (POMC) gene. *Genes Dev.* **10**, 1284-1295.

Lanctôt, C., Lamolet, B. and Drouin, J. (1997). The *bicoid*-related homeoprotein Ptx1 defines the most anterior domain of the embryo and differentiates posterior from anterior lateral mesoderm. *Development* **124**, 2807-2817.

Lanctôt, C., Moreau, A., Chamberland, M., Tremblay, M. L. and Drouin, J. (1999). Hindlimb patterning and mandible development require the *Ptx1* gene. *Development* **126**, 1805-1810.

Langmead, B., Trapnell, C., Pop, M. and Salzberg, S. L. (2009). Ultrafast and memory-efficient alignment of short DNA sequences to the human genome. *Genome Biol.* **10**, R25.

Lerdrup, M., Johansen, J. V., Agrawal-Singh, S. and Hansen, K. (2016). An interactive environment for agile analysis and visualization of ChIP-sequencing data. *Nat. Struct. Mol. Biol.* **23**, 349-357.

Li, D., Sakuma, R., Vakili, N. A., Mo, R., Puviindran, V., Deimling, S., Zhang, X., Hopyan, S. and Hui, C. C. (2014). Formation of proximal and anterior limb skeleton requires early function of Irx3 and Irx5 and is negatively regulated by Shh signaling. *Dev. Cell* **29**, 233-240.

Liao, Y., Smyth, G. K. and Shi, W. (2014). featureCounts: an efficient general purpose program for assigning sequence reads to genomic features. *Bioinformatics* **30**, 923-930.

Litingtung, Y., Dahn, R. D., Li, Y., Fallon, J. F. and Chiang, C. (2002). Shh and Gli3 are dispensable for limb skeleton formation but regulate digit number and identity. *Nature* **418**, 979-983.

Marcil, A., Dumontier, É., Chamberland, M., Camper, S. A. and Drouin, J. (2003). *Pitx1* and *Pitx2* are required for development of hindlimb buds. *Development* **130**, 45-55.

McCarthy, D. J., Chen, Y. and Smyth, G. K. (2012). Differential expression analysis of multifactor RNA-Seq experiments with respect to biological variation. *Nucleic Acids Res.* **40**, 4288-4297.
McLean, C. Y., Bristor, D., Hiller, M., Clarke, S. L., Schaar, B. T., Lowe, C. B., Wenger, A. M. and Bejerano, G. (2010). GREAT improves functional interpretation of cis-regulatory regions. *Nat. Biotechnol.* **28**, 495-501.
Minguillon, C., Del Buono, J. and Logan, M. P. (2005). Tbx5 and Tbx4 are not sufficient to determine limb-specific morphologies but have common roles in initiating limb outgrowth. *Dev. Cell* **8**, 75-84.
Mo, R., Freer, A. M., Zinyk, D. L., Crackower, M. A., Michaud, J., Heng, H. H., Chik, K. W., Shi, X. M., Tsui, L. C., Cheng, S. H. et al. (1997). Specific and redundant functions of Gli2 and Gli3 zinc finger genes in skeletal patterning and development. *Development* **124**, 113-123.
Nagy, A., Gertsenstein, M., Vintersten, K. and Behringer, R. (2009). Alcian blue staining of the mouse fetal cartilaginous skeleton. *Cold Spring Harb. Protoc.* **2009**, pdb.prot5169.
Nelson, C. E., Morgan, B. A., Burke, A. C., Laufer, E., Dimambro, E., Murtaugh, L. C., Gonzales, E., Tessarollo, L., Parada, L. F. and Tabin, C. (1996). Analysis of Hox gene expression in the chick limb bud. *Development* **122**, 1449-1466.
Ohuchi, H., Takeuchi, J., Yoshioka, H., Ishimaru, Y., Ogura, K., Takahashi, N., Ogura, T. and Noji, S. (1998). Correlation of wing-leg identity in ectopic FGF-induced chimeric limbs with the differential expression of chick Tbx5 and Tbx4. *Development* **125**, 51-60.
Ouimette, J.-F., Lavertu Jolin, M., L'honoré, A., Gifuni, A. and Drouin, J. (2010). Divergent transcriptional activities determine limb identity. *Nat. Commun.* **1**, 35.
Papaioannou, V. E. (2014). The T-box gene family: emerging roles in development, stem cells and cancer. *Development* **141**, 3819-3833.
Park, S., Infante, C. R., Rivera-Davila, L. C. and Menke, D. B. (2014). Conserved regulation of hoxc11 by pitx1 in Anolis lizards. *J. Exp. Zool. B Mol. Dev. Evol.* **322**, 156-165.
Petit, F., Sears, K. E. and Ahituv, N. (2017). Limb development: a paradigm of gene regulation. *Nat. Rev. Genet.* **18**, 245-258.
Pieretti, J., Gehrke, A. R., Schneider, I., Adachi, N., Nakamura, T. and Shubin, N. H. (2015). Organogenesis in deep time: a problem in genomics, development, and paleontology. *Proc. Natl. Acad. Sci. USA* **112**, 4871-4876.
Probst, S., Kraemer, C., Demougin, P., Sheth, R., Martin, G. R., Shiratori, H., Hamada, H., Iber, D., Zeller, R. and Zuniga, A. (2011). SHH propagates distal limb bud development by enhancing CYP26B1-mediated retinoic acid clearance via AER-FGF signalling. *Development* **138**, 1913-1923.
Robinson, M. D., McCarthy, D. J. and Smyth, G. K. (2010). edgeR: a Bioconductor package for differential expression analysis of digital gene expression data. *Bioinformatics* **26**, 139-140.
Rodriguez-Esteban, C., Tsukui, T., Yonei, S., Magallon, J., Tamura, K. and Izpisua Belmonte, J. C. (1999). The T-box genes Tbx4 and Tbx5 regulate limb outgrowth and identity. *Nature* **398**, 814-818.
Samuel, C. S., Zhao, C., Bathgate, R. A., Du, X. J., Summers, R. J., Amento, E. P., Walker, L. L., McBurnie, M., Zhao, L. and Tregear, G. W. (2005). The relaxin gene-knockout mouse: a model of progressive fibrosis. *Ann. N. Y. Acad. Sci.* **1041**, 173-181.
Sears, K. E., Capellini, T. D. and Diogo, R. (2015). On the serial homology of the pectoral and pelvic girdles of tetrapods. *Evolution* **69**, 2543-2555.
Shlyueva, D., Stampfel, G. and Stark, A. (2014). Transcriptional enhancers: from properties to genome-wide predictions. *Nat. Rev. Genet.* **15**, 272-286.
Shubin, N., Tabin, C. and Carroll, S. (1997). Fossils, genes and the evolution of animal limbs. *Nature* **388**, 639-648.
Singh, M. K., Petry, M., Haenig, B., Lescher, B., Leitges, M. and Kispert, A. (2005). The T-box transcription factor Tbx15 is required for skeletal development. *Mech. Dev.* **122**, 131-144.
Spielmann, M., Brancati, F., Krawitz, P. M., Robinson, P. N., Ibrahim, D. M., Franke, M., Hecht, J., Lohan, S., Dathe, K., Nardone, A. M. et al. (2012). Homeotic arm-to-leg transformation associated with genomic rearrangements at the PITX1 locus. *Am. J. Hum. Genet.* **91**, 629-635.
Szeto, D. P., Rodriguez-Esteban, C., Ryan, A. K., O'Connell, S. M., Liu, F., Kioussi, C., Gleiberman, A. S., Izpisua-Belmonte, J. C. and Rosenfeld, M. G. (1999). Role of the Bicoid-related homeodomain factor Pitx1 in specifying hindlimb morphogenesis and pituitary development. *Genes Dev.* **13**, 484-494.
Takeuchi, J. K., Koshiba-Takeuchi, K., Matsumoto, K., Vogel-Höpker, A., Naitoh-Matsuo, M., Ogura, K., Takahashi, N., Yasuda, K. and Ogura, T. (1999). Tbx5 and Tbx4 genes determine the wing/leg identity of limb buds. *Nature* **398**, 810-814.
Thorvaldsdottir, H., Robinson, J. T. and Mesirov, J. P. (2013). Integrative Genomics Viewer (IGV): high-performance genomics data visualization and exploration. *Brief. Bioinform.* **14**, 178-192.
Tremblay, J. J., Lanctôt, C. and Drouin, J. (1998). The pan-pituitary activator of transcription, Ptx-1 (pituitary homeobox 1), acts in synergy with SF-1 and Pit1 and is an upstream regulator of the Lim-homeodomain gene Lim3/Lhx3. *Mol. Endocrinol.* **12**, 428-441.
Wellik, D. M. and Capecchi, M. R. (2003). Hox10 and Hox11 genes are required to globally pattern the mammalian skeleton. *Science* **301**, 363-367.
Xu, B. and Wellik, D. M. (2011). Axial Hox9 activity establishes the posterior field in the developing forelimb. *Proc. Natl. Acad. Sci. USA* **108**, 4888-4891.
Zhang, Y., Liu, T., Meyer, C. A., Eeckhoute, J., Johnson, D. S., Bernstein, B. E., Nusbaum, C., Myers, R. M., Brown, M., Li, W. et al. (2008). Model-based analysis of ChIP-Seq (MACS). *Genome Biol.* **9**, R137.
Zhou, X., Lindsay, H. and Robinson, M. D. (2014). Robustly detecting differential expression in RNA sequencing data using observation weights. *Nucleic Acids Res.* **42**, e91.

Supplementary Figures and Tables

Figure S1

A **Multidimensional Scaling (MDS) plots of expression profiling comparisons**

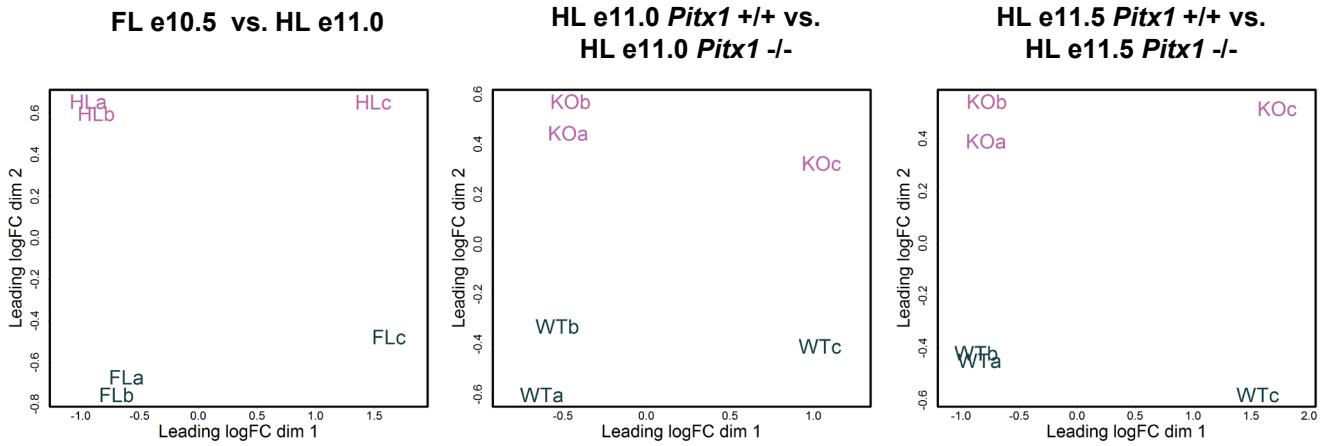

B **Correlation analysis of stage-matched FL e10.5 and HL e11.0 chromatin mark ChIP-seq datasets**

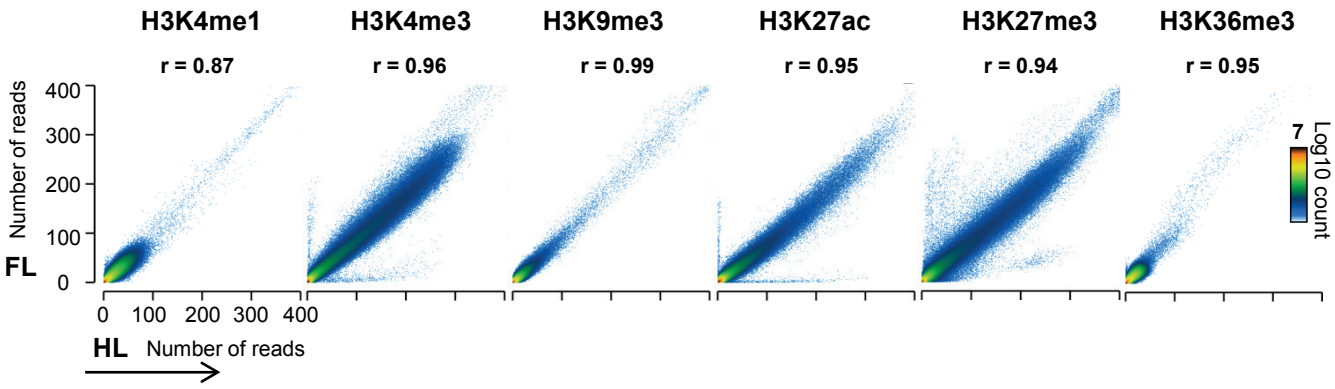

C

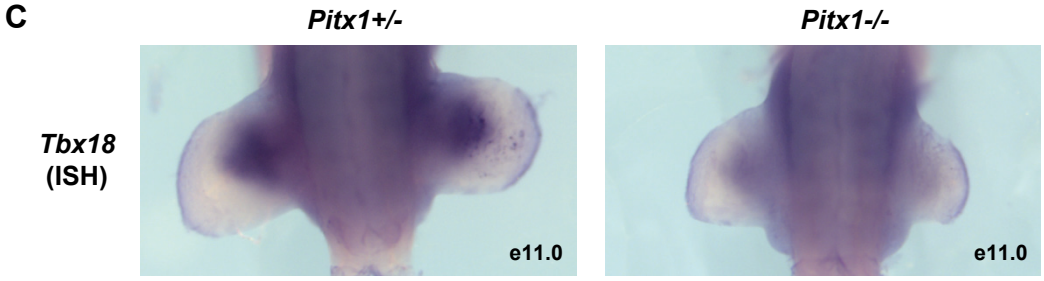

Supplementary Figure S1

A) Multidimensional scaling (MDS) plots of expression profiling analyses by RNA-seq.

B) Correlation analysis of chromatin mark profiles in stage-matched e10.5 FL vs. e11.0 HL. The genome is partitioned into 100 bp bins and the read counts for each mark in each bin are plotted. The Pearson's correlation coefficients are computed using using bins that register more than 50 reads in each sample.

C) In situ hybridization for *Tbx18* on e11.0 *Pitx1+/-* and *Pitx1-/-* HLs.

Figure S2

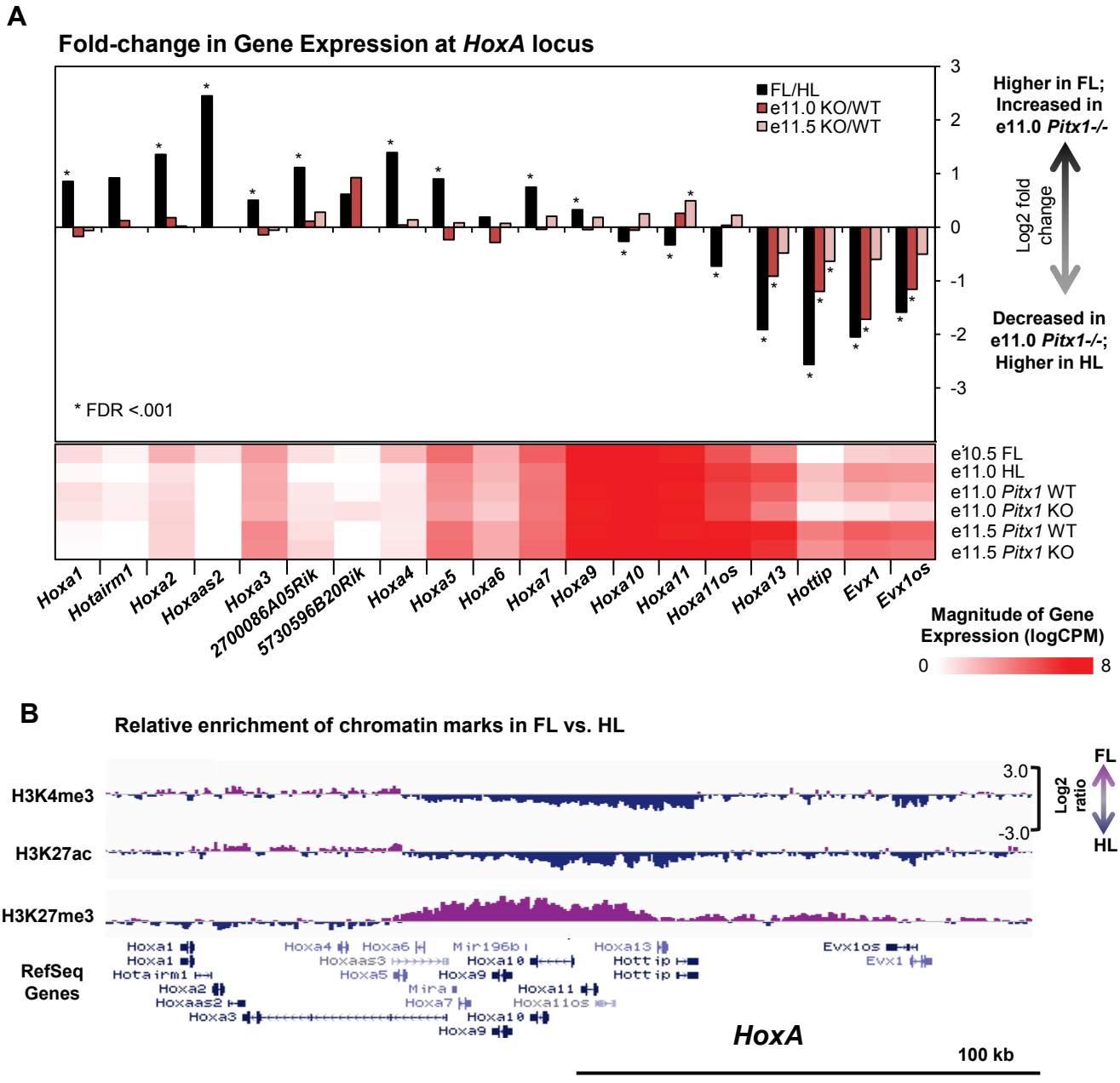

Figure S3

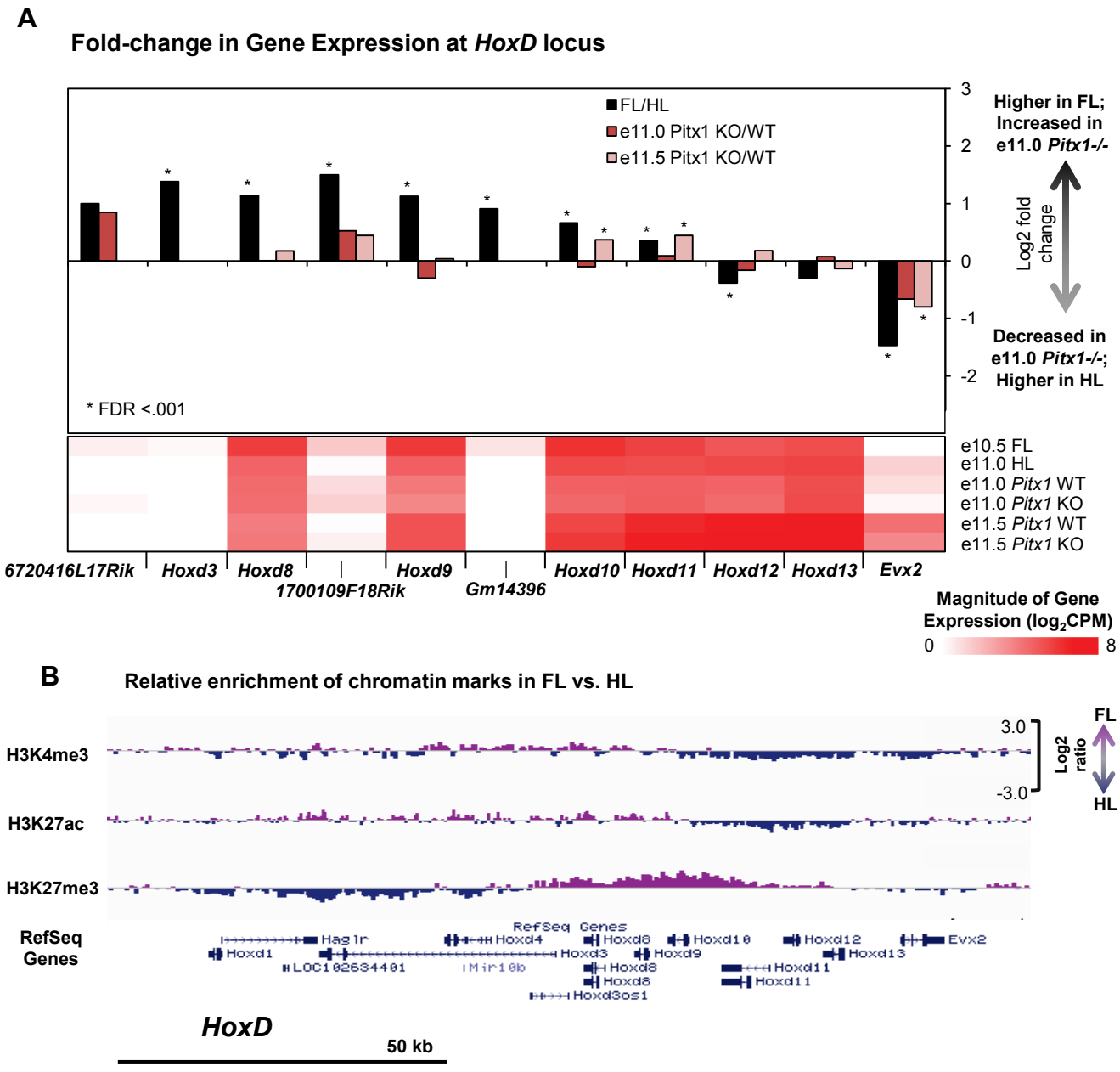

Figure S4

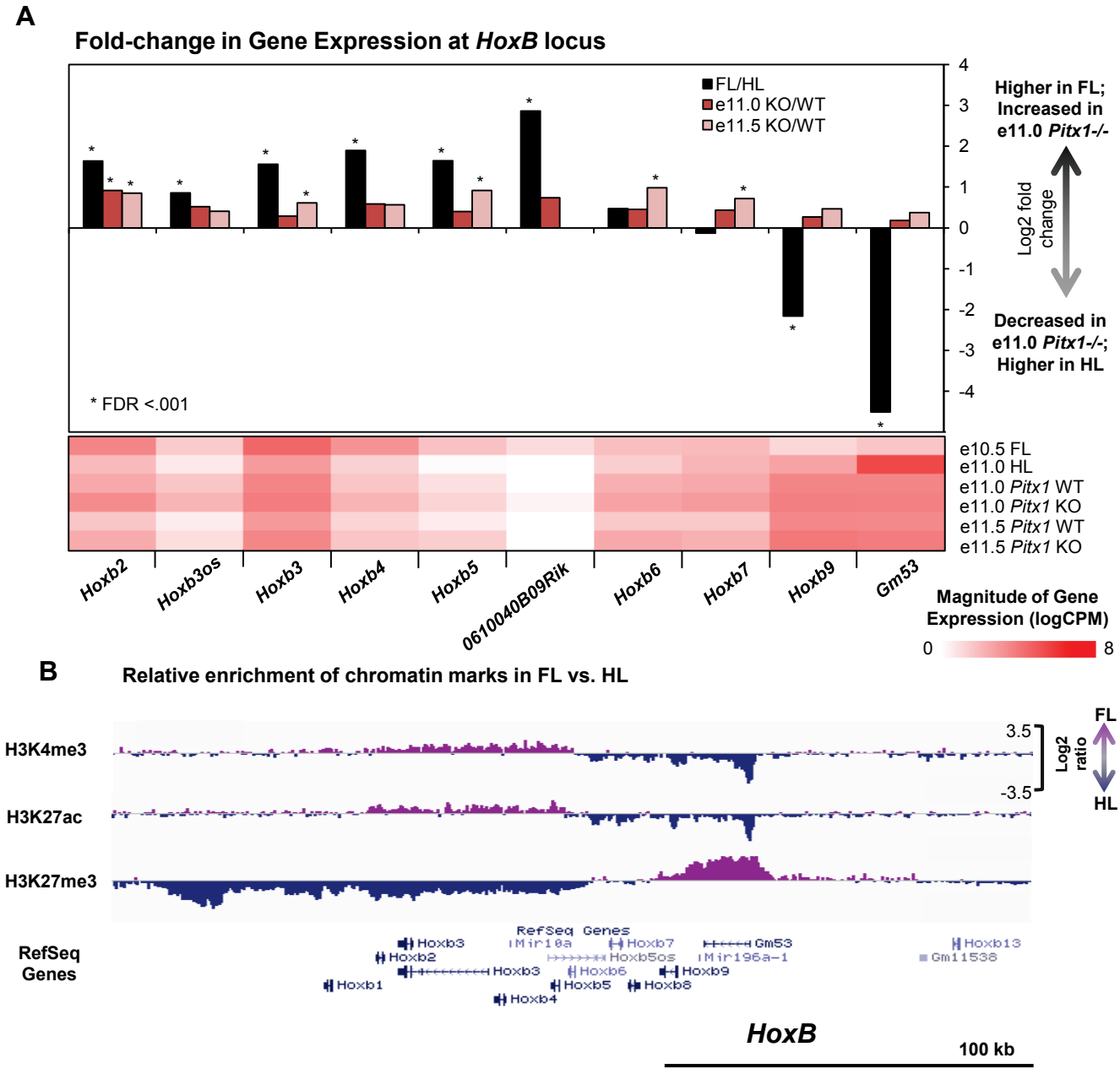

Figure S5

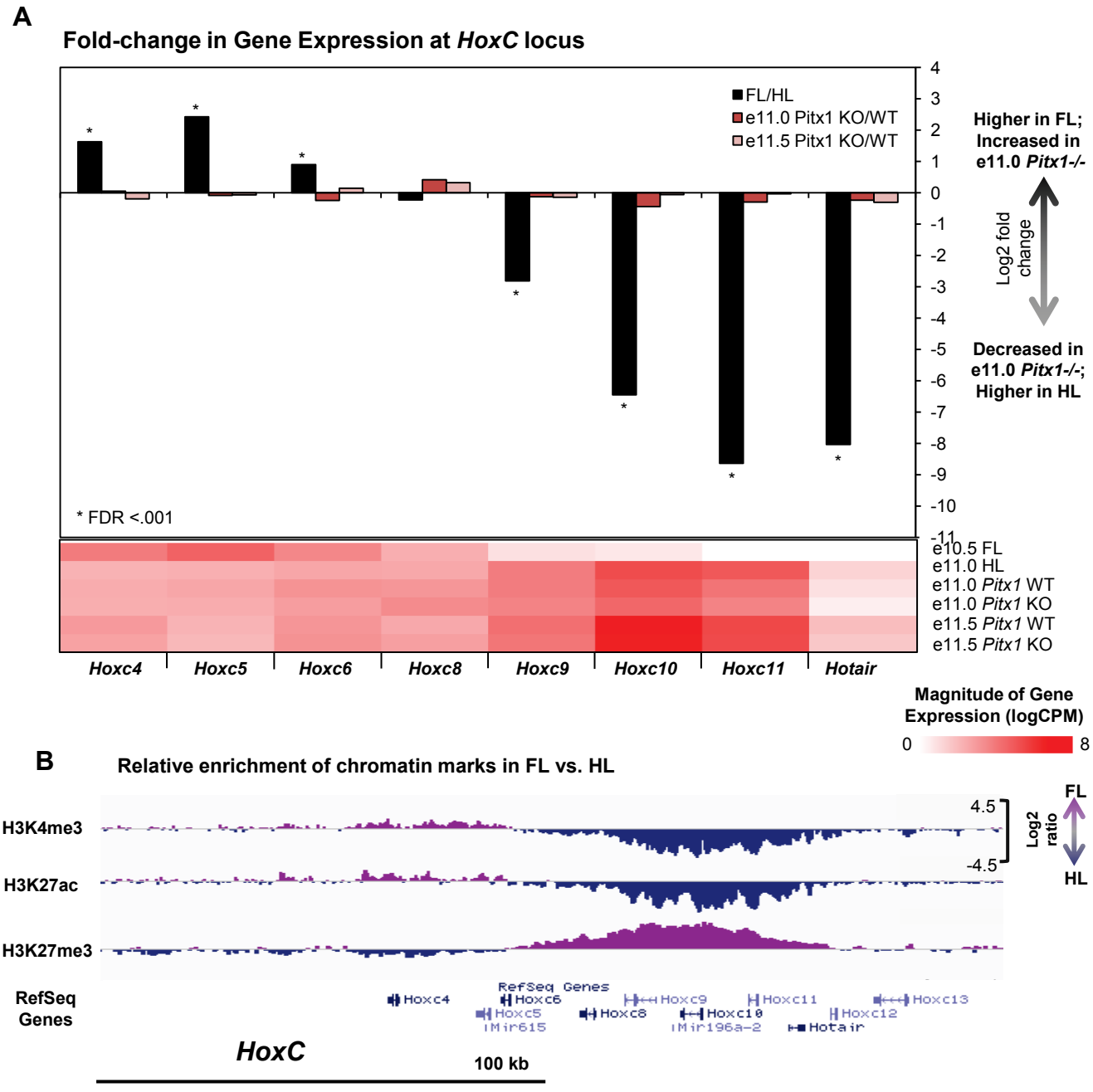

Supplementary Figures S2-S5

A) Log_2 fold-changes in *HoxA-D* gene expression in stage-matched FL vs. HL, e11.0 *Pitx1-/-* vs. wt HL, and e11.5 *Pitx1-/-* vs. wt HL. Below the bar graph of gene expression changes is a heatmap of the magnitude of gene expression in each sample, in log_2 counts per million.

B) The relative enrichment of chromatin mark profiles for H3K4me3, H3K27ac, and H3K27me3 in stage-matched FL vs. HL at the *HoxA-D* loci. These tracks are the log_2 ratios of HL/FL

Supplementary Tables S1-S3

Complementary to Figure 2B: Lists of Pitx1-dependent genes clustered according to limb-type restricted expression.

Table S1 HL-enriched, *Pitx1*-dependent genes at e11.0 – 46 genes

Gene ID	Gene Symbol	log2FC FL/HL	log2FC KO/WT	FDR FL/HL	FDR KO/WT
ENSMUSG00000100096	Gm28760	-8.91	-4.04	2.59E-43	7.42E-19
ENSMUSG00000021506	Pitx1	-9.22	-2.48	0.00E+00	1.09E-130
ENSMUSG00000048747	E130114P18Rik	-2.22	-2.22	1.36E-37	3.78E-19
ENSMUSG00000075334	Rprm	-0.88	-1.72	7.30E-05	8.01E-11
ENSMUSG00000086126	5730457N03Rik	-2.05	-1.72	4.10E-14	4.81E-17
ENSMUSG00000072720	Myo18b	-2.08	-1.65	1.28E-15	2.50E-07
ENSMUSG00000030111	A2m	-1.66	-1.28	1.68E-20	1.19E-07
ENSMUSG00000033965	Slc16a2	-0.75	-1.25	1.46E-16	4.01E-17
ENSMUSG00000052854	Nrk	-0.49	-1.23	6.56E-17	3.56E-23
ENSMUSG00000000094	Tbx4	-4.42	-1.21	0.00E+00	3.29E-24
ENSMUSG00000055408	Gm15053	-2.56	-1.20	6.98E-32	7.53E-06
ENSMUSG00000102373	9530018H14Rik	-1.92	-1.16	3.20E-40	2.51E-08
ENSMUSG00000005503	Evx1	-1.59	-1.16	2.08E-16	5.03E-04
ENSMUSG00000028519	Dab1	-0.66	-1.08	8.31E-04	5.79E-06
ENSMUSG00000061353	Cxcl12	-0.65	-1.07	2.53E-19	6.66E-23
ENSMUSG00000053137	Mapk11	-0.46	-1.00	5.14E-06	6.64E-07
ENSMUSG00000038203	Hoxa13	-1.91	-0.92	2.30E-72	2.48E-06
ENSMUSG00000025743	Sdc3	-0.26	-0.87	6.15E-04	2.04E-08
ENSMUSG00000052581	Lrrtm4	-0.67	-0.87	7.98E-05	7.09E-05
ENSMUSG00000029695	Aass	-0.72	-0.86	2.15E-16	2.09E-09
ENSMUSG00000057777	Mab21l2	-0.47	-0.83	4.66E-17	3.89E-10
ENSMUSG00000061524	Zic2	-0.43	-0.81	3.16E-08	1.12E-10
ENSMUSG00000033618	Map3k13	-0.52	-0.79	6.54E-04	1.63E-04
ENSMUSG00000031654	Cbln1	-0.52	-0.77	4.67E-06	2.83E-04
ENSMUSG00000058145	Adamts17	-0.76	-0.76	3.44E-21	3.94E-07
ENSMUSG00000110874	NA	-1.03	-0.75	3.66E-09	4.65E-05
ENSMUSG00000051177	Plcb1	-0.61	-0.72	4.07E-13	3.60E-07
ENSMUSG00000021253	Tgfb3	-0.53	-0.67	3.81E-11	2.37E-06
ENSMUSG00000021136	Smoc1	-0.40	-0.66	2.87E-09	8.96E-05
ENSMUSG00000051515	Fam181b	-0.64	-0.59	6.57E-16	1.42E-05
ENSMUSG00000004040	Stat3	-0.28	-0.58	2.36E-04	7.52E-05
ENSMUSG00000030351	Tspan11	-0.69	-0.58	1.93E-06	7.69E-04
ENSMUSG00000016763	Scube1	-0.27	-0.57	1.24E-04	5.03E-04
ENSMUSG00000021097	Clmn	-0.34	-0.55	1.49E-03	7.81E-04
ENSMUSG00000036523	Greb1	-0.40	-0.54	7.66E-09	2.56E-04
ENSMUSG00000029622	Arpc1b	-0.57	-0.52	1.20E-14	7.46E-07
ENSMUSG00000023079	Gtf2ird1	-0.46	-0.50	4.43E-14	2.38E-06
ENSMUSG00000020044	Timp3	-0.35	-0.45	1.24E-08	2.60E-04
ENSMUSG00000057315	Arhgap24	-0.44	-0.44	4.83E-07	3.05E-04
ENSMUSG00000038193	Hand2	-0.43	-0.44	1.24E-13	2.47E-05
ENSMUSG00000004631	Sgce	-0.41	-0.43	1.10E-07	2.66E-04
ENSMUSG00000029790	Cep41	-0.35	-0.41	2.01E-08	4.03E-05
ENSMUSG00000056947	Mab21l1	-0.53	-0.40	9.42E-14	4.21E-04
ENSMUSG00000030352	Tspan9	-0.24	-0.40	8.79E-04	7.09E-04
ENSMUSG00000027962	Vcam1	-0.53	-0.38	3.96E-20	2.14E-04
ENSMUSG00000054675	Tmem119	-0.32	-0.34	4.06E-06	2.09E-04

Table S2

A FL-enriched genes with increased expression in *Pitx1-/-* HL – 24 genes

Gene ID	Gene Symbol	log2FC FL/HL	log2FC KO/WT	FDR FL/HL	FDR KO/WT
ENSMUSG00000028023	**Pitx2**	1.36	1.59	8.42E-26	2.39E-16
ENSMUSG00000053117	**E330013P04Rik**	0.85	1.24	4.73E-05	8.34E-13
ENSMUSG00000020297	**Nsg2**	0.89	1.01	2.08E-04	5.07E-06
ENSMUSG00000052504	**Epha3**	1.52	0.96	1.07E-74	3.86E-07
ENSMUSG00000075588	**Hoxb2**	1.64	0.92	1.58E-42	4.18E-10
ENSMUSG00000019894	**Slc6a15**	1.12	0.83	3.94E-07	9.59E-04
ENSMUSG00000046318	**Ccbe1**	0.72	0.81	4.44E-03	1.58E-04
ENSMUSG00000043969	**Emx2**	1.03	0.78	2.93E-19	1.95E-12
ENSMUSG00000022309	**Angpt1**	0.36	0.78	5.10E-03	1.02E-12
ENSMUSG00000033981	**Gria2**	2.52	0.67	1.70E-68	2.30E-05
ENSMUSG00000041920	**Slc16a6**	0.69	0.66	2.01E-05	2.39E-04
ENSMUSG00000025592	**Dach2**	0.41	0.64	7.19E-03	6.73E-04
ENSMUSG00000025856	**Pdgfa**	0.27	0.58	5.61E-03	1.35E-10
ENSMUSG00000024087	**Cyp1b1**	1.01	0.56	7.34E-09	7.84E-05
ENSMUSG00000067931	**Zfp948**	0.35	0.54	3.49E-03	4.22E-07
ENSMUSG00000073988	**Ttpa**	0.45	0.50	2.95E-05	1.36E-05
ENSMUSG00000025921	**Rdh10**	0.36	0.49	2.01E-05	3.81E-05
ENSMUSG00000040464	**Gtpbp10**	0.22	0.49	9.54E-03	2.36E-06
ENSMUSG00000031558	**Slit2**	0.56	0.47	5.06E-19	8.80E-05
ENSMUSG00000026739	**Bmi1**	0.28	0.46	5.14E-03	2.44E-07
ENSMUSG00000045103	**Dmd**	0.65	0.44	4.64E-18	1.42E-04
ENSMUSG00000031299	**Pdha1**	0.28	0.43	3.04E-05	1.84E-05
ENSMUSG00000074519	**Etohi1**	0.43	0.42	2.54E-05	8.75E-04
ENSMUSG00000037720	**Tmem33**	0.27	0.37	1.90E-03	8.55E-05

B HL-enriched genes with increased expression in *Pitx1-/-* HL – 11 genes

Gene ID	Gene Symbol	log2FC FL/HL	log2FC KO/WT	FDR FL/HL	FDR KO/WT
ENSMUSG00000034009	**Rxfp1**	-7.66	1.13	3.90E-93	7.09E-26
ENSMUSG00000031636	**Pdlim3**	-1.87	1.02	6.66E-16	1.51E-12
ENSMUSG00000065232	**Gm22973**	-0.34	0.91	5.52E-03	6.31E-15
ENSMUSG00000048138	**Dmrt2**	-0.87	0.90	4.78E-07	2.15E-11
ENSMUSG00000073940	**Hbb-bt**	-1.57	0.85	3.37E-16	2.03E-04
ENSMUSG00000052305	**Hbb-bs**	-1.37	0.84	4.24E-16	5.19E-08
ENSMUSG00000032033	**Barx2**	-0.73	0.64	2.56E-04	1.32E-05
ENSMUSG00000019987	**Arg1**	-0.49	0.61	2.25E-04	1.39E-06
ENSMUSG00000058258	**Idi1**	-0.36	0.60	9.23E-03	6.73E-08
ENSMUSG00000042258	**Isl1**	-3.55	0.56	2.09E-139	4.72E-05
ENSMUSG00000021508	**Cxcl14**	-0.48	0.40	1.01E-10	8.54E-04

Table S3 FL-enriched, *Pitx1*-dependent genes at e11.0 – 39 genes

Gene ID	Gene Symbol	log2FC FL/HL	log2FC KO/WT	FDR FL/HL	FDR KO/WT
ENSMUSG00000047793	**Sned1**	0.75	-1.67	2.20E-12	3.31E-32
ENSMUSG00000039153	**Runx2**	2.36	-1.65	2.72E-49	2.53E-05
ENSMUSG00000053141	**Ptprt**	0.64	-1.60	5.89E-04	8.47E-07
ENSMUSG00000062713	**Sim2**	1.62	-1.41	6.27E-58	4.38E-05
ENSMUSG00000042607	**Asb4**	0.40	-1.26	5.21E-06	6.04E-38
ENSMUSG00000004872	**Pax3**	0.65	-1.25	1.58E-14	3.17E-12
ENSMUSG00000049538	**Adamts16**	0.72	-1.19	4.44E-06	4.01E-09
ENSMUSG00000025216	**Lbx1**	0.60	-1.17	1.13E-10	5.08E-05
ENSMUSG00000031285	**Dcx**	0.44	-1.16	3.30E-06	1.46E-25
ENSMUSG00000047759	**Hs3st3a1**	0.97	-0.95	2.58E-21	9.71E-05
ENSMUSG00000020218	**Wif1**	0.51	-0.94	1.23E-06	8.08E-09
ENSMUSG00000032852	**Rspo4**	1.99	-0.90	5.00E-96	4.98E-05
ENSMUSG00000019230	**Lhx9**	0.40	-0.80	2.01E-08	1.77E-25
ENSMUSG00000025584	**Pde8a**	0.68	-0.79	2.32E-06	1.20E-04
ENSMUSG00000030029	**Lrig1**	0.35	-0.75	3.05E-04	2.32E-08
ENSMUSG00000052951	**C130021I20Rik**	0.22	-0.74	2.08E-03	7.61E-11
ENSMUSG00000038765	**Lmx1b**	0.24	-0.72	2.07E-03	3.97E-07
ENSMUSG00000038119	**Cdon**	0.52	-0.71	9.67E-12	2.49E-12
ENSMUSG00000067276	**Capn6**	0.31	-0.69	2.92E-04	5.87E-11
ENSMUSG00000037138	**Aff3**	0.40	-0.67	4.70E-09	1.55E-08
ENSMUSG00000042961	**Egflam**	0.39	-0.66	2.66E-05	1.07E-04
ENSMUSG00000021318	**Gli3**	0.46	-0.64	1.35E-12	1.32E-06
ENSMUSG00000032035	**Ets1**	0.19	-0.64	9.22E-03	4.43E-07
ENSMUSG00000070407	**Hs3st3b1**	0.80	-0.63	7.78E-36	7.14E-07
ENSMUSG00000032332	**Col12a1**	0.28	-0.55	1.88E-04	2.25E-07
ENSMUSG00000026147	**Col9a1**	0.48	-0.54	2.01E-11	1.29E-06
ENSMUSG00000096054	**Syne1**	0.32	-0.54	5.08E-03	5.95E-07
ENSMUSG00000052331	**Ankrd44**	0.52	-0.50	1.07E-17	1.65E-04
ENSMUSG00000042594	**Sh2b3**	0.28	-0.49	1.05E-03	8.17E-04
ENSMUSG00000054263	**Lifr**	0.38	-0.49	7.94E-08	1.59E-04
ENSMUSG00000027833	**Shox2**	0.21	-0.49	4.35E-03	2.58E-06
ENSMUSG00000022231	**Sema5a**	0.33	-0.48	5.32E-08	8.49E-04
ENSMUSG00000001300	**Efnb2**	0.33	-0.47	2.88E-06	7.31E-05
ENSMUSG00000032846	**Zswim6**	0.22	-0.46	7.34E-03	2.22E-05
ENSMUSG00000063564	**Col23a1**	0.27	-0.42	1.18E-05	7.46E-05
ENSMUSG00000029231	**Pdgfra**	0.30	-0.42	7.85E-04	1.82E-04
ENSMUSG00000035245	**Eogt**	0.25	-0.40	8.21E-04	4.97E-04
ENSMUSG00000047786	**Lix1**	0.48	-0.39	1.77E-11	1.78E-04
ENSMUSG00000037605	**Lphn3**	0.43	-0.38	4.55E-10	8.64E-04